

SCREENING OF PLANT-MEDIATED NANOPARTICLES FOR ANTIFUNGAL ACTIVITY



UNIVERSITY *of the*
WESTERN CAPE

Irving de Beer

A mini-thesis submitted in partial fulfilment of the requirements for the degree
Magister Scientiae in Nanoscience
Department of Biotechnology
University of the Western Cape

Supervisor: Dr Ashwil Klein
Co-supervisor(s): Prof Mervin Meyer
Prof Abram Madiehe
December 2020

ABSTRACT

Screening of plant-mediated nanoparticles for antifungal Properties

MSc Mini-thesis, Department of Biotechnology, University of the Western Cape

I. W. de Beer

Nanotechnology is spreading rapidly across the world as an extremely powerful technology. Nanoscience and nanotechnology are innovative scientific advancements that have been introduced only in this century. Nanotechnology has developed as the scientific advancement to grow and transform the entire agri-food area, with the potential to elevate global food production, in addition to the nutritional value, quality, and safety of food and food products. It has gained recognition due to its variability in shape, size, and dimension and how it correlates to its possibilities. One of those functions is nanoparticles' (NPs) ability to have antimicrobial activity, more specifically its antifungal activity. One particular pathway of synthesising NPs is through phytonanotechnology which is the use of biomaterial to synthesise the NPs. In this study leaf extracts from *Salvia hispanica* (Chia) were used to synthesise gold (Au) and silver (Ag) NPs. Various plant concentrations were used as well as two different temperatures (25 and 70 °C) to determine NP formation. After synthesis, the NPs were characterised by UV-vis spectroscopy (UV-vis), Dynamic Light Scattering (DLS) and High-resolution transmission electron microscopy (HRTEM). Based on the characterisation of the NPs, the leaf extract proved to be successful for both Au- and AgNPs. UV-vis spectroscopy confirmed uniformity of the nanoparticles as well as wavelength formation that is specific to Au and Ag nanoparticles respectively. The DLS was used to determine the hydrodynamic size of the NPs as well as numerically quantifying the uniformity of the NPs. HRTEM was used to visually confirm the size, shape and dimension of the NPs synthesised. In addition, AgNPs synthesised from *Salvia hispanica*, *Salvia Africana-lutea* and *Cotyledon orbiculata-l* including the plant extracts from *Salvia hispanica* were used to screen for antifungal activity against *Fusarium oxysporum*. The results showed that potential antifungal activity was only observed for the NPs synthesised from *Salvia hispanica*

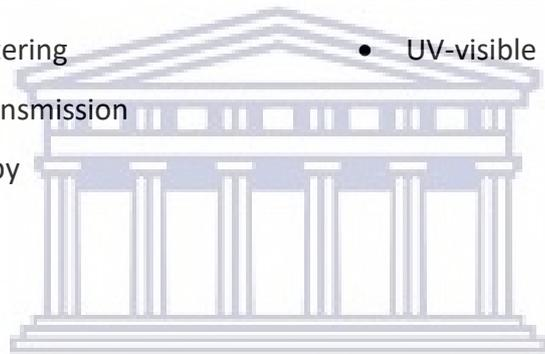
Screening of plant-mediated nanoparticles for antifungal Properties

I. W. de Beer

plant extract whereas the other NPs did not produce any antifungal activity against *F. oxysporum*.

KEYWORDS:

- Antifungal activity
- Antimicrobial activity
- Biogenic/Green Synthesis
- Dynamic light scattering
- High-resolution transmission electron Microscopy
- Hydrodynamic size
- Phytochemical
- Silver nanoparticles
- UV-visible spectroscopy



UNIVERSITY *of the*
WESTERN CAPE



UNIVERSITY of the
WESTERN CAPE

University of the Western Cape

Private Bag X17, Bellville 7535, South Africa

Telephone: ++27-21- 959 2255/959 2762 Fax: ++27-21- 959 1268/2266

Email: joanbeverdonker@uwc.ac.za

FACULTY OF NATURAL SCIENCE

GENERAL PLAGIARISM DECLARATION

Name: ...Irving de Beer.....

Student number: ...3438901.....

1. I hereby declare that I know what plagiarism entails, namely to use another's work and to present it as my own without attributing the sources in the correct way. (Refer to University Calendar part 1 for definition)
2. I know that plagiarism is a punishable offence because it constitutes theft.
3. I understand the plagiarism policy of the Faculty of Natural Science of the University of the Western Cape.
4. I know what the consequences will be if I plagiarise in any of the assignments for my course.
5. I declare therefore that all work presented by me for every aspect of my course, will be my own, and where I have made use of another's work, I will attribute the source in the correct way.

I W de Beer

Signature

29 November 2020

Date

Acknowledgement

I would like to pay a tribute to the following people for their respective influence and the part they've played in this study period:

To Dr Klein for being my supervisor, thank you very much for this opportunity I truly am grateful for the chance you've given me.

To my co-supervisors Prof Meyer and Prof Madiehe, thank you for facilitating my studies and allowing me access to what was needed for the project.

To the proteomics lab, thank you for any assistance I needed. I truly appreciate it.

To the NIC labs for aiding me almost every single step of the way and a special mention to Yamkela and Abdul. Ensuring that whatever I did was thorough, and thank you for all your assistance.

To the nanoscience students that joined the program with me in nanobiomed, thank you for the priceless memories.

To my parents for being my pillar of support, as well as my brother, I thank you dearly.

To all my friends that have been there to support me through my ups and downs thank you very much I am so thankful.

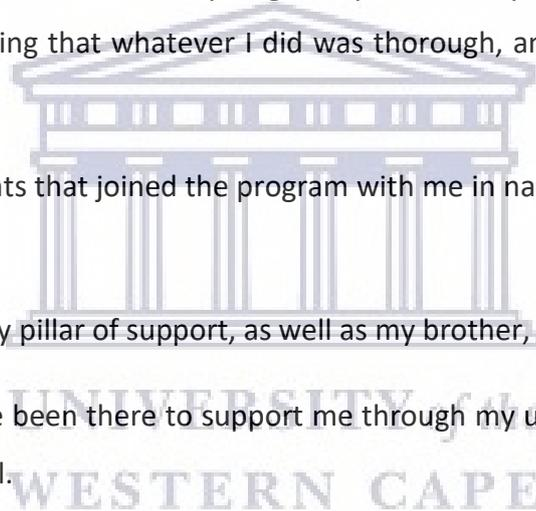
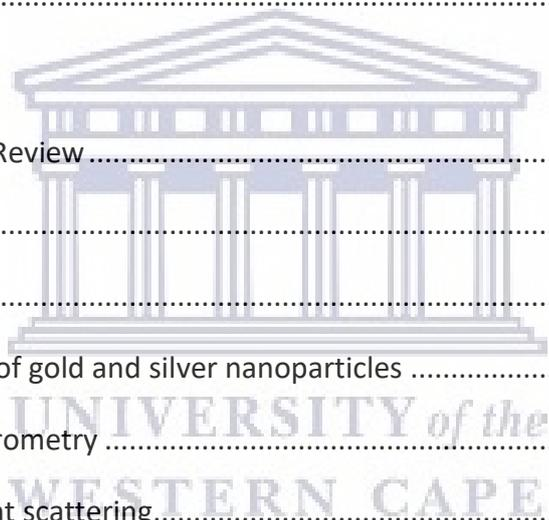
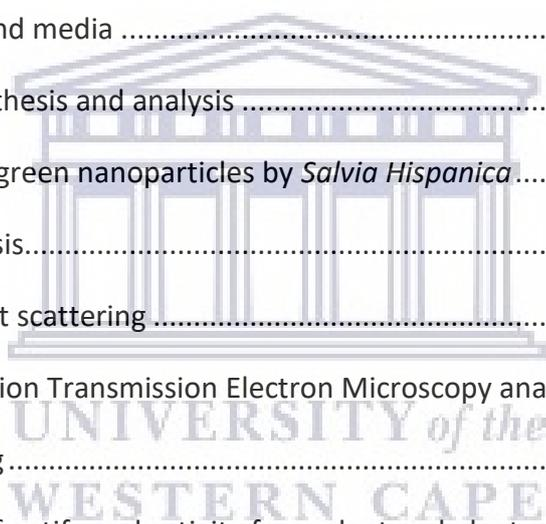


Table of contents

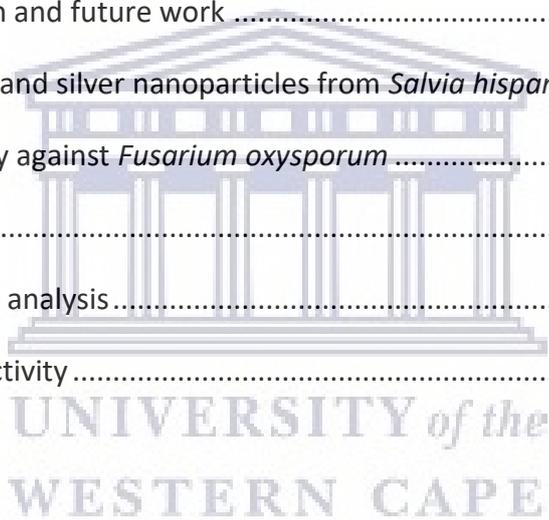
ABSTRACT.....	i
KEYWORDS.....	ii
Acknowledgement.....	i
Table of contents.....	ii
List of Figures:.....	v
List of tables.....	vii
List of Abbreviations:.....	viii
1 Chapter I: Literature Review.....	1
1.1 Introduction.....	1
1.2 Nanotechnology.....	2
1.3 Characterisation of gold and silver nanoparticles.....	3
1.3.1 UV-vis spectrometry.....	3
1.3.2 Dynamic Light scattering.....	4
1.3.3 High resolution transmission Electron Microscopy analysis.....	5
1.4 Silver Nanoparticles (AgNPs).....	6
1.5 Gold nanoparticles (AuNPs).....	7
1.6 Antimicrobial nanoparticles.....	8
1.7 Phytochemicals of plants.....	12
1.7.1 <i>Salvia</i> species.....	13
1.7.2 <i>Cotyledon orbiculata</i> L.....	14
1.8 Pathogenic Fungi.....	15
1.8.1 <i>Fusarium</i> species.....	16



1.9	Farm maintenance	18
1.10	Research Proposal	18
1.10.1	Problem statement	18
1.10.2	Aims.....	19
1.10.3	Objectives of the study	19
2	Chapter II: Material and methods.....	20
2.1	Reagents and suppliers	20
2.2	Equipment and service providers	20
2.3	Stock solutions and media	21
2.4	Nanoparticle synthesis and analysis	21
2.4.1	Synthesis of green nanoparticles by <i>Salvia Hispanica</i>	21
2.4.2	UV-vis analysis.....	22
2.4.3	Dynamic light scattering	22
2.4.4	High-Resolution Transmission Electron Microscopy analysis.....	23
2.5	Antifungal testing	23
2.5.1	Evaluation of antifungal activity from plant and plant mediated NPs	23
3	Chapter III: Biogenic synthesis and characterisation of gold and silver nanoparticles from <i>Salvia hispanica</i> L. leaf extracts	24
3.1	Introduction.....	24
3.2	Results and Discussion	25
3.2.1	Synthesis and characterisation	25
3.2.2	UV-vis spectrometry	25
3.2.3	Dynamic Light scattering (DLS)	27
3.2.4	Transmission Electron Microscopy (TEM) analysis.....	29



4	Chapter IV: Antifungal activities of plant extracts and plant-mediated silver nanoparticles	31
4.1	Introduction.....	31
4.2	Results and Discussion	32
4.2.1	Positive control (Carbendazim) against <i>Fusarium oxysporum</i>	32
4.2.2	Antifungal activity of plant extracts.....	33
4.2.3	Antifungal activity of plant derived AgNPs	34
5	Chapter V: Conclusion and future work	36
5.1	Synthesis of gold and silver nanoparticles from <i>Salvia hispanica</i>	36
5.2	Antifungal activity against <i>Fusarium oxysporum</i>	36
5.3	Future works	36
5.3.1	Nanoparticle analysis	36
5.3.2	Antifungal activity	36
	Reference List.....	38



List of Figures:

Figure 1.1: Different synthesis routes for nanoparticles (Adapted from Mittal <i>et al.</i> , 2013).	2
Figure 1.2: UV-Vis absorption spectra depicting the uniformity band in AuNPs (Adapted from Elbagory <i>et al.</i> , 2016).	4
Figure 1.3: Dynamic light scattering distribution of AuNPs depicting the hydrodynamic diameter (Adapted from Elbagory <i>et al.</i> , 2017).....	5
Figure 1.4: High resolution Transmission Electron Microscopy image of AuNPs at 10nm (A) and its Selected area electron diffraction pattern (B) (Adapted from Elbagory <i>et al.</i> , 2017).	6
Figure 1.5: Types of metal nanoparticles and their applications (Mittal <i>et al.</i> , 2013).	7
Figure 1.6: Types of shapes that may be obtained from gold nanoparticles (Adapted from Alaqad and Saleh, 2016).	8
Figure 1.7: Depiction of the broad usability of nanoparticles in terms of antimicrobial properties. Acronyms: NP = Nanoparticles. PPE = Personal Protective equipment (Adapted from Yah and Simate, 2015).	9
Figure 1.8: The process through which a nanoparticle is synthesised, from its ionic state (Mittal <i>et al.</i> , 2013).	13
Figure 1.9: Depiction of the disease cycle in plants (Adapted from Zeilinger <i>et al.</i> , 2016).	16
Figure 1.10: An adapted image of <i>Fusarium oxysporum</i> , A) Macrocondia and B) Microconidia. Scale Bar: 25 μm (Leslie and Summerell, 2006).	17
Figure 2.1: Preparation of Plant-extract material. The image of the <i>Salvia hispanica</i> plant was received (Adapted from Mohd Ali <i>et al.</i> , 2012).....	22
Figure 3.1: Visual representation of the colour changes associated with AgNP formation across a plant extract concentration gradient.....	25
Figure 3.2: UV-vis of silver nanoparticles at various plant extract concentrations. Nanoparticles were synthesised at 25 $^{\circ}\text{C}$ (A) and 70 $^{\circ}\text{C}$ (B) respectively. AgNPs synthesis from leaf extracts at different concentrations (A-B).	26

Figure 3.3: UV-Vis of gold nanoparticles at various plant extract concentrations. Nanoparticles were synthesised at 25 °C (A) and 70 °C (B) respectively. AuNPs synthesis from leaf extracts at different concentrations (A-B).27

Figure 3.4: Transmission Electron Microscopy for silver nanoparticles. A) Silver Nanoparticles that were viewed 50 nm as per the scale depicted by the scale bar in the bottom left. This depicts uniformity in the size of the nanoparticles however non-uniform in shape. B) This displays the crystallinity at 2 nm as depicted by the scale bar in the bottom left corner. C) This is the SAED patterns that depict the diffraction rings of FCC Ag.29

Figure 3.5: Transmission Electron Microscopy for gold nanoparticles. A) Gold Nanoparticles that were viewed 50 nm as per the scale depicted by the scale bar in the bottom left. This depicts uniformity in the size of the nanoparticles however non-uniform in shape. B) This displays the crystallinity at 2 nm as depicted by the scale bar in the bottom left corner. C) This is the SAED patterns that depict the diffraction rings of FCC Au.30

Figure 4.1: Antifungal activity of carbendazim against *F. oxysporum*. Mycelial growth was restricted in a concentration dependent manner. Carbendazim at 0.1 mg/ml restricted mycelial growth to 45 mm whereas 0.2 mg/ml and 0.3 mg/ml completely inhibited mycelial growth on PGA plates after 7 days at 30 °C.33

Figure 4.2: Antifungal activity of *Cotyledon orbiculata* var. *oblonga* extract, *Salvia Africana-lutea* extract and *Salvia hispanica* extracts against *F. oxysporum*. No changes in mycelial growth were observed in response to different concentration (4 mg/ml and 10 mg/ml) of plant extract. All samples incubated for 7 days at 30 °C34

Figure 4.3: Well diffusion antiungal activity assay of *Cotyledon orbiculata* var. *oblonga*, *Salvia Africana-lutea* and *Salvia hispanica* L. derived AgNPs against *F. oxysporum*. The fungus was allowed to grow for 7 days at 30 °C. No significant reduction in mycelial growth was measured in response to AgNPs from *Cotyledon orbiculata* var. *oblonga* and *Salvia Africana-lutea*. Fungal mycelial growth reduction was observed in response to AgNPs synthesised from *Salvia hispanica* L.35

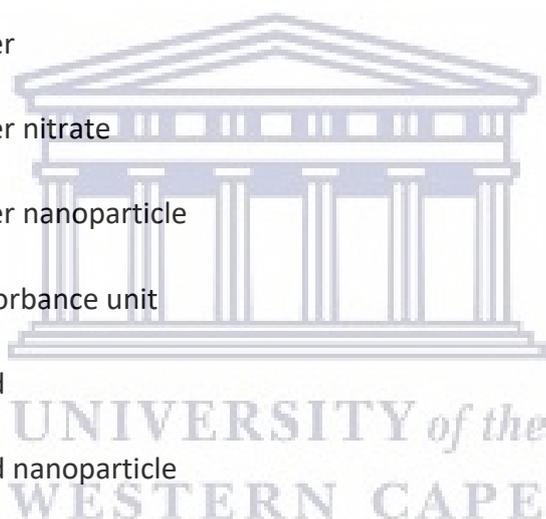
List of tables

Table 1.1: Nanoparticles that have been tested against different microbes for antimicrobial activity	10
Table 2.1: List of Reagents used in the investigation	20
Table 2.2: Laboratory equipment used.....	20
Table 2.3: Constituents and stock solutions used	21
Table 3.1: Dynamic light analysis of gold and silver Nanoparticles. Which is the average size of the silver and gold nanoparticles.	28

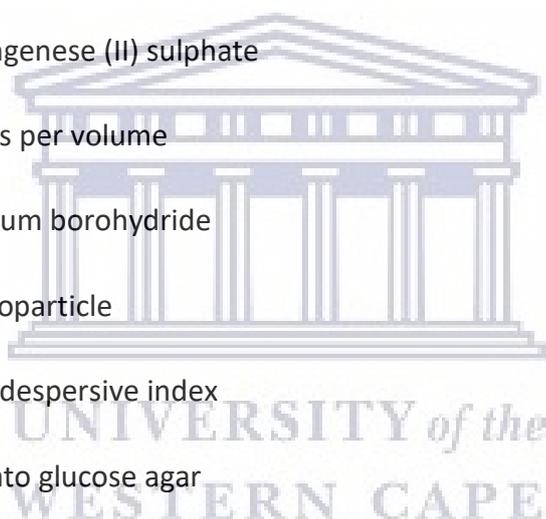


List of Abbreviations:

±:	Approximately
%:	Percent
°C:	Degree Celsius
λ max:	Lambda max
μl:	Microlitre
1D:	One-Dimensional
3D:	Three-Dimensional
Ag:	Silver
AgNO ₃ :	Silver nitrate
AgNP:	Silver nanoparticle
au:	Absorbance unit
Au:	Gold
AuNP:	Gold nanoparticle
Ca(NO ₃) ₂ .4H ₂ O:	Calcium nitrate tetrahydrate
CCD:	Charge-coupled device
dH ₂ O:	Deionised water
DLS:	Dynamic light scattering
EtOH:	Ethanol
FCC:	Face-centred cubic
FeCl ₃ :	Iron (III) chloride
HAuCl ₄ :	Chloroauric acid



HRTEM:	High resolution transmission electron microscopy
KH_2PO_4 :	Monopotassium phosphate
kV:	Kilovolts
mg:	Milligrams
mg/ml:	Milligrams per millilitre
MIC:	Minimum inhibitory concentration
ml:	Millilitre
mM:	MilliMolar
MnSO_4 :	Mangenes (II) sulphate
m/v:	Mass per volume
NaBH_4 :	Sodium borohydride
NP:	Nanoparticle
PDI:	Polydispersive index
PGA:	Potato glucose agar
PPE:	Personal protective equipment
rpm:	Rotations per minute
SAED:	Selected area electron diffraction
SnCl_2 :	Tin (II) chloride
v/v:	Volume per volume
UV-vis:	Ultraviolet-visible



1 Chapter I: Literature Review

1.1 Introduction

Green synthesis is a type of synthesis route that is used in nanoscience in order to create nanoparticles (NPs). This method is a simple one step reaction that is highly cost-effective. The method is a reproducible choice of synthesis and the material that is produced is highly stable (Mittal *et al.*, 2014). In nanoscience, methodology approaches are either: top-down or bottom-up synthesis approaches, whereby the nanomaterial can be made through either breaking down bulk material or by self-assembly (Mittal *et al.*, 2013). Nanomaterial has been identified to have its own range of beneficial properties which is due to their chemical, physical, electronic, and magnetic properties which are not exact to their bulk material and/or atoms or molecules (Rad *et al.*, 2011).

Silver (Ag) NPs have a wide range of applications of which antimicrobial activity is one of them (Alaqad and Saleh, 2016), which include antifungal activity (Kim *et al.*, 2012). Gold (Au) NPs have been noted to have low toxicity while having a high surface area. This becomes useful in biomedical applications. Furthermore AuNPs are also capable of binding to other molecules, being modified, which are useful within biochemistry due to its compatibility and optical properties (Alaqad and Saleh, 2016). Other NPs demonstrated to have antifungal activity include gold, selenium and copper NPs. Plant species are known to have resistance to a broad spectrum of pathogens which is why the majority of their microbial relationships are either symbiotic or neutral whereby parasitic infections are the exception (Staskawicz, 2001). Crop loss is an issue concerning the agricultural farming industry of which it may be a quantitative or qualitative loss. Moreover, the quantitative loss is associated with crop loss due to pests (Savary *et al.*, 2018).

In this review, the use of green nanotechnology will be discussed and its' value-added to antifungal microbes, specifically fungus that has a detrimental effect on farm yield and compromise farm yield.

1.2 Nanotechnology

In nanoscience, there are two main approaches as to how NPs are synthesised. The two approaches are classified as either: Top-down or bottom-up. What this means is that nanomaterial is either synthesised by dividing bulk material into the nanoscale range or undergoing a process that allows for the assembly of nanomaterial from ions (Figure 1.1) (Mittal *et al.*, 2013). There are three methods of synthesis that exist for metal NPs synthesis namely: Physical, chemical, and biological. Examples of physical synthesis are Ball milling and chemical etching whereby bulk material is broken down into material that is sized in the nano-range. Chemical synthesis such as chemical precipitation and vapour deposition making use of the self-assembly. The use of self-assembly, a bottom-up method, also occurs with biological synthesis. Biological synthesis, also known as biogenic or green synthesis, is an approach to making NPs and this process makes use of organic matter i.e., plant extract material is taken from various parts of the plant such as its leaves or roots or using microorganisms or the synthesis of the nanomaterial (Alaqad and Saleh, 2016). Nanomaterial itself have their criteria of dimensions ranging from one-Dimensional (1D) to three-Dimensional (3D) whereby 1D nanomaterial are seen to be at least <100 nm in size and often spherical in shape (Delgado-Ramos, 2014).

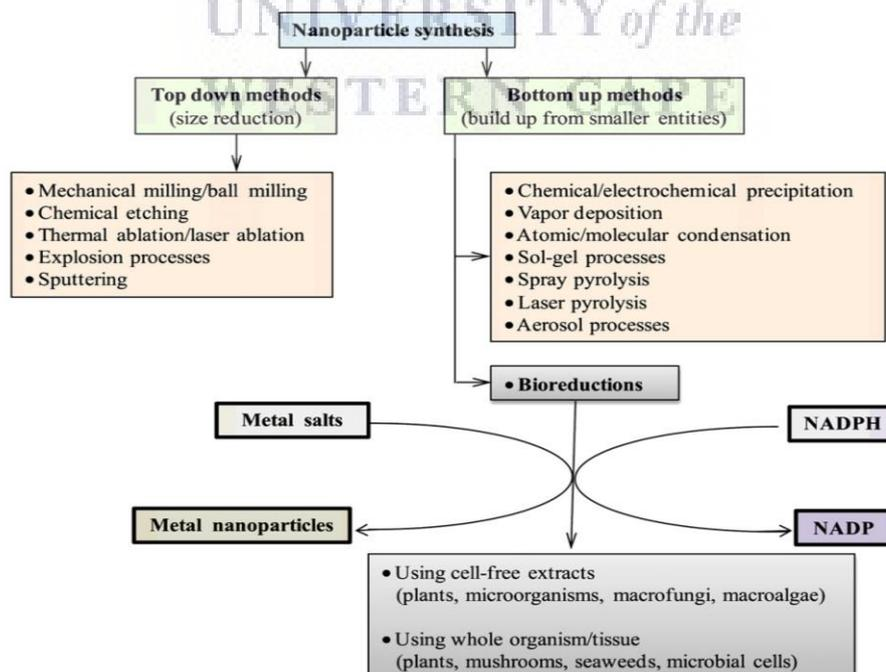


Figure 1.1: Different synthesis routes for nanoparticles (Adapted from Mittal *et al.*, 2013).

1.3 Characterisation of gold and silver nanoparticles

When working with nanomaterial a crucial component coupled to the synthesis is the subsequent characterisation that occurs. The reason for characterising the synthesised NPs to confirm the actual synthesis of the NPs and its size, shape, and uniformity. The instruments that are capable of this are UV-visible spectrometry (UV-vis), Dynamic light scattering (DLS) and High resolution transmission electron microscopy (HRTEM/TEM) (Elbagory *et al.*, 2016; Alaqad and Saleh, 2016; Mittal *et al.*, 2013).

1.3.1 UV-vis spectrometry

The use of UV-vis for characterisation is for identification, confirmation as well as the initial check of uniformity (Alaqad and Saleh, 2016). It is a beneficial instrument for understanding electronic transition of species that capable of absorbing frequencies from near infrared throughout the visible light range through to the UV region of the electromagnetic spectrum. This occurs with transition energy within the range between 10^2 and 10^3 kJmol^{-1} (Amendola and Meneghetti, 2009). Metal NPs have an absorption band within this spectrum which is due to the coherent oscillation of the metal's respective conduction band free electrons that are being induced due to its interaction with electromagnetic field, which can be defined as surface plasmon resonance (SPR). This band is known to be a characteristic for metallic NPs and is not observed within its respective bulk metal's absorption (Olenic *et al.*, 2016; Hu *et al.*, 2006). This means that because each nanomaterial such as Au- or AgNP have their own SPR, the material will be identified and confirmed through a peak in the graph occurring at a particular wavelength. Moreover, the shape and bend of the curve can be seen as the preliminary confirmation of uniformity (Alaqad and Saleh, 2016). Furthermore, based on literature a peak for AgNPs can be observed around 400 nm and the literature confirms that the peak on UV-vis for AuNPs is around 520 nm (Alaqad and Saleh, 2016). Figure 1.2 is a depiction of a uniform curve obtained for AuNPs.

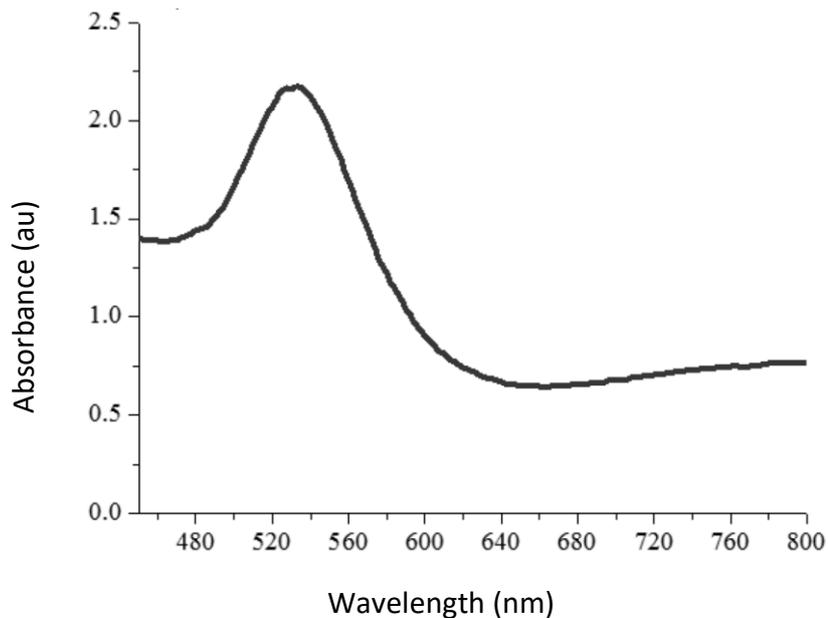


Figure 1.2: UV-Vis absorption spectra depicting the uniformity band in AuNPs (Adapted from Elbagory *et al.*, 2016).

1.3.2 Dynamic Light scattering

Dynamic light scattering (DLS) is a characterisation tool, also known as photon correlation spectrometry that is often coupled with other characterisation techniques such as UV-Vis and TEM. This is because the function of DLS to determine the hydrodynamic average particle size of NPs whilst suspended in liquid media as well as their polydispersive index (PDI) (Mittal *et al.*, 2013; Hoo *et al.*, 2008). The NPs are analysed as the light gets scattered off from them, which then results in localised variations within the refractive index of the solution (Hoo *et al.*, 2008). The PDI must have a numeric value close or less than 0.7, as greater than 0.7 is indicative of a broad size distribution within the respective sample and is not ideal for DLS measurement (Noruzi, 2015). As Literature further states that DLS is an ideal instrument to use for monomodal samples (Hoo *et al.*, 2008) which is initially confirmed by the peak of UV-vis. DLS, therefore, is used as further confirmation of uniformity as well as the size of the synthesised nanoparticles and to confirm the size range of the NPs being within the nanometre range. Figure 1.3 is indicative of the size range of the two respective gold nanoparticles from a study conducted by Elbagory *et al.* (2017).

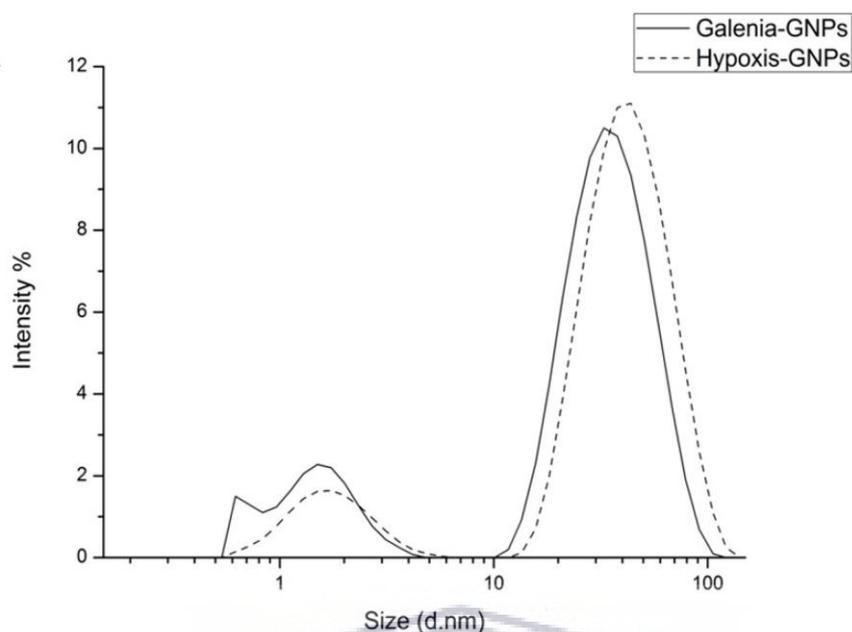


Figure 1.3: Dynamic light scattering distribution of AuNPs depicting the hydrodynamic diameter (Adapted from Elbagory *et al.*, 2017).

1.3.3 High resolution transmission Electron Microscopy analysis

In a review by Alaqad and Saleh (2016), it was recorded that the functions of HRTEM are to determine morphology, shape, crystallography, and particle size. This is because TEM is a visual tool and it is possible to see the NPs to scale. It measures the interaction of transmitted electrons whilst being passed towards a thin layer of the respective specimen. This is achieved because electron beams are focused via magnetic lenses onto the specimen which is resting on a metal grid. The electrons are either absorbed or they are scattered by the specimen. This interaction by the electrons and the specimen is noted by a detector which is capable of generating an image that is able to be seen through a charge-coupled device (CCD) camera (Figure 1.4) (Wang, 2001). Lastly HRTEM is also able to determine the selected area electron diffraction (SAED) patterns of the NPs which is used as further confirmation of the respective metal as they depict with their diffraction rings index that confers to its face-centred cubic (FCC) (Joe *et al.*, 2017; Elbagory *et al.*, 2016).

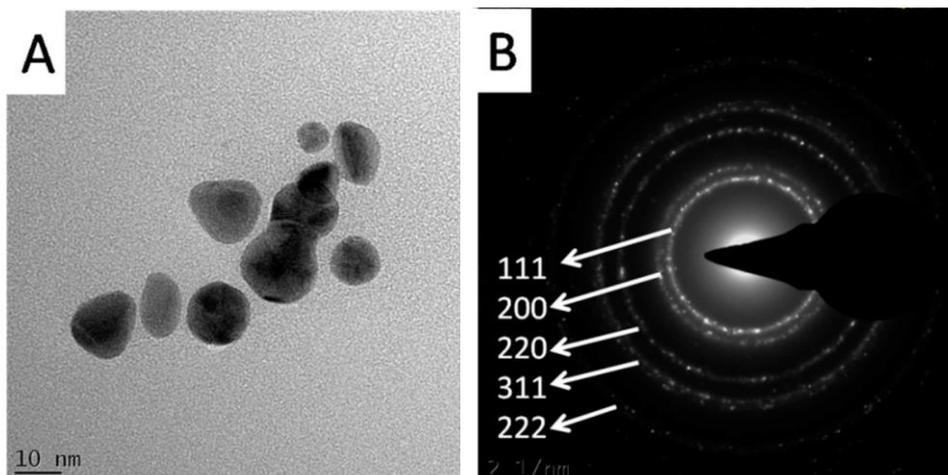


Figure 1.4: High resolution Transmission Electron Microscopy image of AuNPs at 10nm (A) and its Selected area electron diffraction pattern (B) (Adapted from Elbagory et al., 2017).

1.4 Silver Nanoparticles (AgNPs)

Ag has become a major contender in the commercialisation of nanomaterial with a value 500 tons of AgNPs being produced per year, with that value expecting to increase (Ahmed *et al.*, 2016; Larue *et al.*, 2014). AgNPs have been studied to have several functions including being chemically stable, having well catalytically active activity and they possess antimicrobial activity (Figure 1.5) (Alaqad and Saleh, 2016). Furthermore, due to their individual plasmon optical spectra it is often applied in biosensing (Alaqad and Saleh, 2016). In a study conducted by Venkatpurwar and Pokharkar (2011) AgNPs that were synthesised were found to have greater toxicity to gram-positive bacteria when its toxicity was compared to gram-negative bacteria which indicates variability in the toxicity of AgNPs for bacteria however triggering inquisitiveness for its toxicity against fungi. The antimicrobial properties are further dependent on the conditions under which it was made such as the pH and ionic strength as well as the actual capping agent (Ahmed *et al.*, 2016). One factor that is suggested to contribute to Ag's antimicrobial activity is the positive charge of Ag^+ ions, and Ag changes from an inert substance to being ionised once it comes into contact with moisture (Klueh *et al.*, 2000). Furthermore, Ag^+ ions are capable of interacting with nucleic acids to form complexes as well as interacting with nucleosides (Ahmed *et al.*, 2016). When considering shaking in the process of synthesis Kaur *et al.* (2018) reported a change in the range of AgNPs synthesised. It was reported that under shaking conditions the size range was between 5 - 20 nm and 10 - 40 nm when the reaction was conducted under static conditions. Furthermore, in this study AgNPs were synthesised from *Pleurotus florida* in a

biogenic synthesis route using microorganisms and underwent characterisation of the NPs such as size analysis mentioned and antimicrobial testing. See Table 1.1 for reference to NPs and their antimicrobial activity against microorganisms albeit bacteria or Fungi.

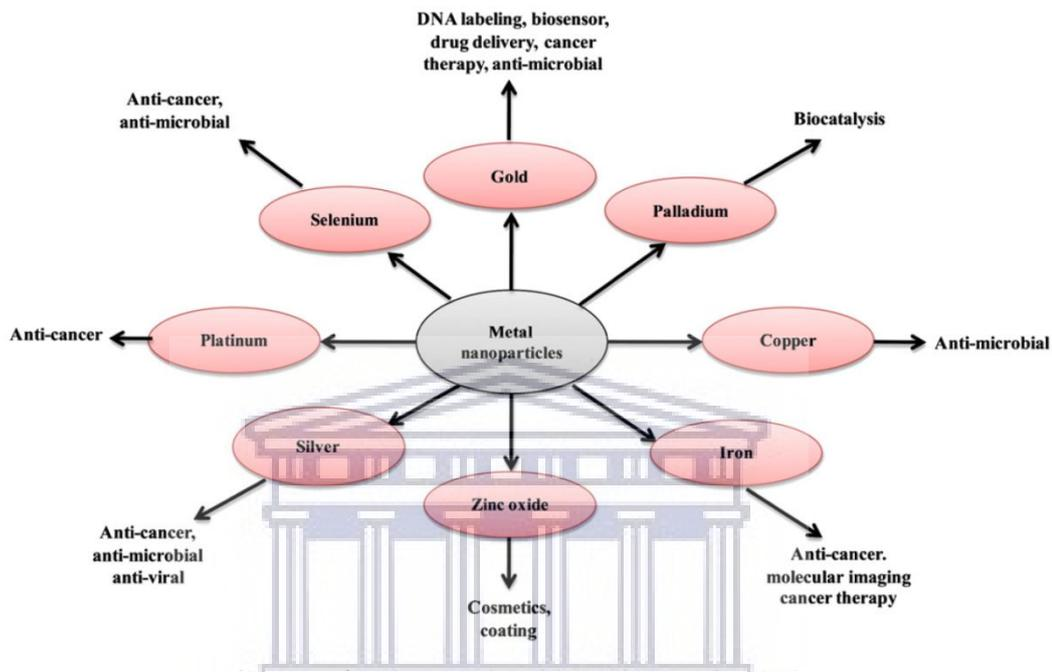


Figure 1.5: Types of metal nanoparticles and their applications (Mittal *et al.*, 2013).

UNIVERSITY of the
WESTERN CAPE

1.5 Gold nanoparticles (AuNPs)

Metal nanoparticles when observed are smaller enough in size in comparison to its bulk material yet they still contain enough units when compared to its respective atoms or molecules that they too differ. Therefore nanomaterial can be observed to have its own range of useful properties due to their chemical, physical, and electronic and magnetic properties which are not the same as its respective bulk material and/or atoms or molecules (Rad *et al.*, 2011). AuNPs once prepared can are wine-red in colour within the solution it was prepared in (Alaqad and Saleh, 2016). Upon analysis of size and shape, it is confirmed that the size range of AuNPs can range from 1 nm to 8 μ m, moreover the type of shapes that can be observed are nanoclusters, spherical, nanorods, star-shaped, nanoshell, branched or nanocubed (Figure 1.6). AuNPs have a low toxicity with a high surface area for the usage of biomedical applications. Furthermore AuNPs are capable of being used to bind to other

molecules for modification purposes that are beneficial within the biochemistry sector due to its compatibility and optical properties (Alaqad and Saleh, 2016). Due to the size of nanoclusters they are capable of being introduced to tissue, cells, and biomolecules such as proteins and DNA (Alaqad and Saleh, 2016). In a study conducted by Jayaseelan *et al.* (2013) biogenic synthesis of AuNP through seed aqueous extract of *Abelmoschus esculentus* were tested for antifungal properties against fungi namely: *Aspergillus flavus*, *Aspergillus niger*, *Candida albicans* and *Puccinia graminis tritici*. The AuNP showed to have antifungal activity for the in vitro well-diffusion assay. This can be viewed on Table 1.

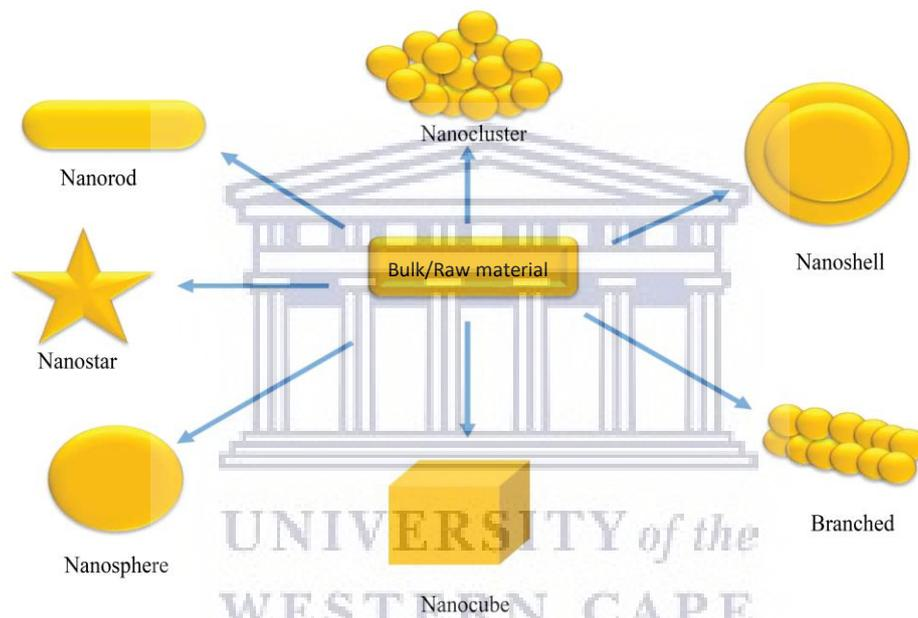


Figure 1.6: Types of shapes that may be obtained from gold nanoparticles (Adapted from Alaqad and Saleh, 2016).

1.6 Antimicrobial nanoparticles

In the review by Mittal *et al.* (2013) gold, selenium, copper as well as silver have been reported to have antimicrobial properties (Figure 1.5), moreover Yah and Simate (2015) goes on to explain which species are categorised under the term antimicrobial and goes on to explain antimicrobial applications (Figure 1.7). The term microbial refers to viruses, bacteria, fungi, and protozoa. Ahmad *et al.* (2013) confirmed the antifungal activity of AuNPs that were synthesised via a crystallisation technique known as the solvothermal method. The strains that were used were three clinical strains of *Candida* which shown the NPs had size-dependent antifungal activity. The reducing agents that were used in the study

were tin (II) chloride (SnCl_2) and Sodium borohydride (NaBH_4) respectively. Shakibaie *et al.* (2015) synthesised selenium NPs using green synthesis, more specifically via a *Bacillus* species Msh-1, and was found to have antifungal activity against *Aspergillus fumigatus* and *Candida albicans*, respectively. Kalatehjari *et al.* (2015) found that colloidal copper NPs have antifungal properties against *Saprolegnia* species that grew on white fish (*Rutilus frisii kutum*) eggs. Lastly, Kim *et al.* (2012) tested three different types of AgNPs against a variety of fungi to confirm the antifungal properties of AgNPs. All three samples were colloidal and had a size range of 7 - 25 nm.

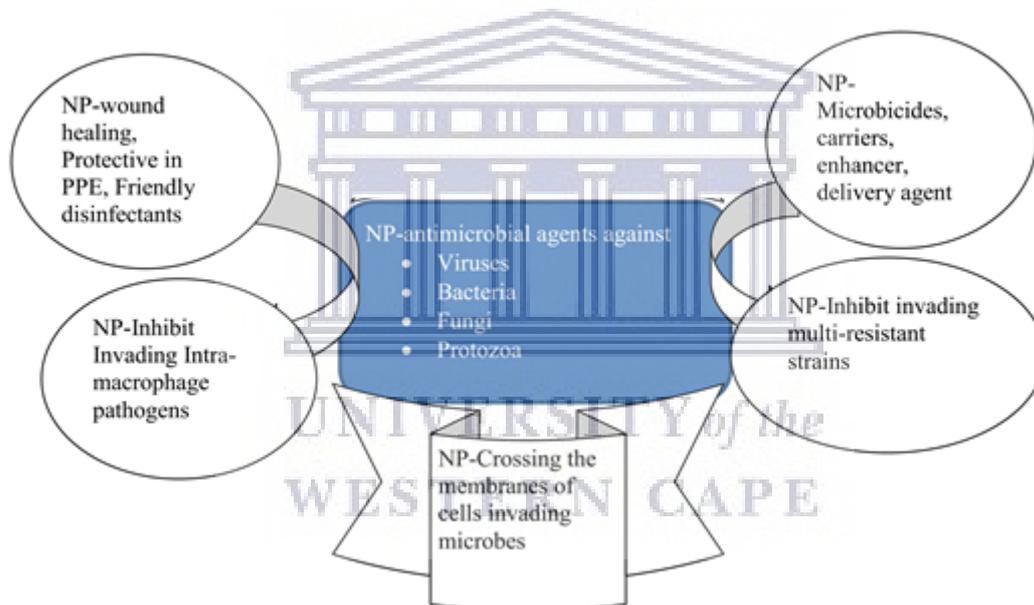


Figure 1.7: Depiction of the broad usability of nanoparticles in terms of antimicrobial properties. Acronyms: NP = Nanoparticles. PPE = Personal Protective equipment (Adapted from Yah and Simate, 2015).

Table 1.1: Nanoparticles that have been tested against different microbes for antimicrobial activity

Antimicrobial Activity	Nanoparticle	Synthesis Route	Shape	Size	Reference
Bacteria:					
<i>Aeromonas hydrophila</i>	Silver	Biogenic: <i>Pleurotus florida</i>	-	5-20nm and 10-40nm	(Kaur <i>et al.</i> , 2018)
<i>Bacillus cereus</i>	Silver	Biogenic: <i>Pleurotus florida</i>	-	5-20nm and 10-40nm	(Kaur <i>et al.</i> , 2018)
<i>Shigella flexneri</i>	Silver	Biogenic: <i>Pleurotus florida</i>	-	5-20nm and 10-40nm	(Kaur <i>et al.</i> , 2018)
<i>Staphylococcus</i>	Silver	Biogenic: <i>Pleurotus florida</i>	-	5-20nm and 10-40nm	(Kaur <i>et al.</i> , 2018)
<i>Yersinia enterocolitica</i>	Silver	Biogenic: <i>Pleurotus florida</i>	-	5-20nm and 10-40nm	(Kaur <i>et al.</i> , 2018)
Fungi:					
<i>Alternaria alternata</i>	Silver	-	Colloidal	7-25nm	(Kim <i>et al.</i> , 2012)
<i>Alternaria brassicicola</i>	Silver	-	Colloidal	7-25nm	(Kim <i>et al.</i> , 2012)
<i>Alternaria solani</i>	Silver	-	Colloidal	7-25nm	(Kim <i>et al.</i> , 2012)
<i>Aspergillus flavus</i>	Gold	Biogenic: <i>Abelmoschus esculentus</i> (seed extract)	Colloidal		(Jayaseelan <i>et al.</i> , 2013)
<i>Aspergillus fumigatus</i>	Selenium	Biogenic: <i>Bacillus</i>	Spherical	120-140nm	(Shakibaie <i>et al.</i> , 2015)
<i>Aspergillus niger</i>	Gold	Biogenic: <i>Abelmoschus esculentus</i> (seed extract)	Colloidal		(Jayaseelan <i>et al.</i> , 2013)
<i>Botrytis cinerea</i>	Silver	-	Colloidal	7-25nm	(Kim <i>et al.</i> , 2012)
<i>Candida</i> species	Gold	Solvothermal	Spherical	7 and 15nm	(Ahmad <i>et al.</i> , 2013)
<i>Candida albicans</i>	Selenium	Biogenic: <i>Bacillus</i>	Spherical	120-140nm	(Shakibaie <i>et al.</i> , 2015)

	Gold	Biogenic: <i>Abelmoschus esculentus</i> (seed extract)	Colloidal		(Jayaseelan <i>et al.</i> , 2013)
<i>Cladosporium cucumerinum</i>	Silver	-	Colloidal	7-25nm	(Kim <i>et al.</i> , 2012)
<i>Corynespora cassiicola</i>	Silver	-	Colloidal	7-25nm	(Kim <i>et al.</i> , 2012)
<i>Colletotrichum gloeosporioides</i>	Cobalt Ferrite	-	Spherical	25nm	(Sharma <i>et al.</i> , 2017)
	Nickel Ferrite	-	Spherical	25nm	(Sharma <i>et al.</i> , 2017)
<i>Cylindrocarpon destructans</i>	Silver	-	Colloidal	7-25nm	(Kim <i>et al.</i> , 2012)
<i>Dematophora necatrix</i>	Cobalt Ferrite	-	Spherical	25nm	(Sharma <i>et al.</i> , 2017)
	Nickel Ferrite	-	Spherical	25nm	(Sharma <i>et al.</i> , 2017)
<i>Didymella bryoniae</i>	Silver	-	colloidal	7-25nm	(Kim <i>et al.</i> , 2012)
<i>Fusarium oxysporum</i> f. sp. <i>cucumerinum</i>	Silver	-	Colloidal	7-25nm	(Kim <i>et al.</i> , 2012)
<i>F. oxysporum</i> f. sp. <i>lycopersici</i>	Silver	-	Colloidal	7-25nm	(Kim <i>et al.</i> , 2012)
<i>F. oxysporum</i>	Silver	-	Colloidal	7-25nm	(Kim <i>et al.</i> , 2012)
	Cobalt Ferrite	-	Spherical	25nm	(Sharma <i>et al.</i> , 2017)
	Nickel Ferrite	-	Spherical	25nm	(Sharma <i>et al.</i> , 2017)
<i>Fusarium solani</i>	Silver	-	Colloidal	7-25nm	(Kim <i>et al.</i> , 2012)
<i>Fusarium</i> sp.	Silver	-	Colloidal	7-25nm	(Kim <i>et al.</i> , 2012)
<i>Glomerella cingulata</i>	Silver	-	Colloidal	7-25nm	(Kim <i>et al.</i> , 2012)
<i>Monosporascus</i>	Silver	-	Colloidal	7-25nm	(Kim <i>et al.</i> ,

<i>cannonballus</i>					2012)
<i>Pythium aphanidermatum</i>	Silver	-	Colloidal	7-25nm	(Kim <i>et al.</i> , 2012)
<i>Pythium spinosum</i>	Silver	-	Colloidal	7-25nm	(Kim <i>et al.</i> , 2012)
<i>Saprolegnia species</i>	Copper	-	Colloidal	-	(Kalatehjari <i>et al.</i> , 2015)
<i>Stemphylium lycopersici</i>	Silver	-	Colloidal	7-25nm	(Kim <i>et al.</i> , 2012)

1.7 Phytochemicals of plants

In chemistry, the perspective of using green-chemistry outweighs non-green chemical processes and this is also identified within the industry of nanotechnology as biogenic synthesis, or phyto-nanotechnology and has been noted to be more environmentally friendly in synthesis when toxicity is compared to other synthesis methods (Thuesombat *et al.*, 2014). The Green synthesis method has been reported to be simple, able to be done in one step and cost-effective. Furthermore, this method has been seen to be reproducible and material that is produced has been seen noted to be stable (Mittal *et al.*, 2014). A further benefit to using plant matter for synthesis is due to it being able to contain both the reducing agent and the stabilising agent (Figure 1.8) required to make the NPs, this due to various concentrations of plant extract each containing their own organic reducing agents for the reduction and capping of the metal (Kumar and Yadav, 2009). How green synthesis is done is by having the plant extract in an aqueous solution to which the metal salt is added. Ahmed *et al.* (2016) managed to synthesise from *Azadirachta indica* in aqueous solutions at various volumes of plant extract: 1, 2, 3, 4 and 5 ml at AgNO₃ concentrations ranging from 1 mM to 5 mM. When preparing plant extract plant material is used at a w/v ratio of 1:10. This can often be done at room temperature (Mittal *et al.*, 2013).

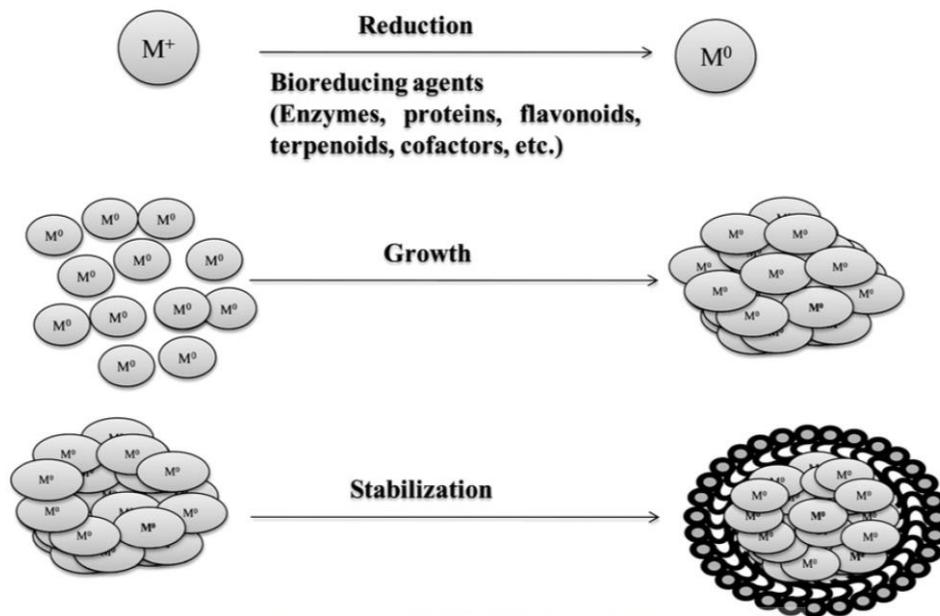


Figure 1.8: The process through which a nanoparticle is synthesised, from its ionic state (Mittal *et al.*, 2013).

1.7.1 *Salvia* species

The largest genus to derive from the family *Lamiaceae*, comprising of approximately 1000 species, is noted to being the *Salvia* plant species (also known as Sage). The origin of its name in Latin, *salvare* means healing properties (Topçu, 2006). This plant species is cultivated in a vast array of areas such as South Africa, Central and South America, Asia as well as the Mediterranean regions. These plants have been utilised for their flavouring agents and aromatics, aesthetics as well as in the cosmetic industry. Moreover, the *Salvia* species is vastly known for its medicinal uses especially within the sphere of traditional medicine (Topçu, 2006). Within the *Salvia* Species, a variety of terpenoids and phenolic compounds are present. Terpenoids present are essential oils and di- and tri-terpenes, whereas the phenolic compounds comprise of flavonoids and caffeic acid derivatives which are known to be situated in the topical regions of the plant (Wu *et al.*, 2012). Furthermore, the plant has been deduced to contain several secondary metabolites (Wu *et al.*, 2012).

1.7.1.1 *Salvia Hispanica* L.

This is a plant species that is grown biannually and is well known for its active ingredients which include essential fatty acids. This plant species is specifically native to South America

and is recognized for its medicinal uses and it is also where it received its common name from Chia (Jamboonsri *et al.*, 2012). The phytochemicals present within Chia has been identified to have variability in concentration due to the conditions in which the plant itself grows. These conditions include cultivation conditions, temperature, as well as the availability of nutrients (Mohd Ali *et al.*, 2012).

1.7.1.2 *Salvia Africana-lutea* L.

The Western Cape region of South Africa is home to a wide variety of plant species known to for their traditional and medicinal purposes. *Salvia Africana-lutea* L is one of those species (Amabeoku *et al.*, 2001). The plant can be found both in the wild as well as in various nature reserves within the Western Cape. *Salvia Africana-lutea* L. is locally known as the “geelblom-salie” which is a common name for the plant in the Afrikaans language (Amabeoku *et al.*, 2001; Watt and Breyer-Brandwijk, 1962). The plant itself has been used for use of treating colds and is also recorded to be a diaphoretic (Watt and Breyer-Brandwijk, 1962). Furthermore, the Nama people of the Cape made use of the decoction of the plant to treat coughs and female ailments (Watt and Breyer-Brandwijk, 1962). The plant has also been tested to have antimicrobial activity bacterial cells namely: *Escherichia coli*, *Staphylococcus aureus* as well as *Microsporum audouinii* (Nielsen *et al.*, 2012). The antifungal activity of *Salvia Africana-lutea* L against various *Fusarium* species have been confirm by a metabolic profiling study conducted by Nkomo *et al.* (2014) who conducted metabolic profiling on *Salvia Africana-lutea* L. Therefore, *Salvia Africana-lutea* L is an ideal candidate for the green synthesis of AgNPs for antifungal activity.

1.7.2 *Cotyledon orbiculata* L.

From the family *Crassulaceae*, stems the genus and species *Cotyledon orbiculata* L., this is an angiosperm which bares red flowering plants with the leaves being a shade of grey-green (James, 1963). Due to it being native to South Africa, a republic that is multilingual, the plant may be referred to by many names, such as Honde-oor, Varkens-ore, Pig ears, Phewula, Seredile and Oorlamsplakkie. Locally by the isiXhosa inhabitants of South Arica, the leaf juice would be warmed and used as ear drops and used specifically for ear drops and the juice was also used to treat toothache (James, 1963).

1.8 Pathogenic Fungi

The role of Fungi in the ecosystem as well as within modern agriculture has become pivotal due to their nutritional versatility and its influence on plant growth and development. They are regarded as vital decomposers and organic recyclers of organic matter. However, fungi serve dual purposes in nature by being either beneficial or detrimental to the roots and atypical regions of various plant species (Zeilinger *et al.*, 2016; Horwitz *et al.*, 2013). Plants are generally resistant to a wide range of pathogens which is why most of their microbial relationships are noted to be symbiotic or neutral except for parasitic infections (Staskawicz, 2001). Moreover, the health of a plant species is highly reliant on the microbial activity that is situated within the rhizosphere as well as on the microbes that are involved with the plant directly (Zeilinger *et al.*, 2016). It has however been recorded that 70-80 % of all diseases that occur within the plant species are due to fungal infections and there are about 10 000 different fungal species that can be defined as pathogenic (Agrios, 2005).

According to Zeilinger *et al.* (2016) the pathogen-host interaction represented as the disease cycle is described in 7 steps (Figure 1.9).

1. The period is defined as the fungal spread whereby the fungus moves via various factors in order to make contact with the plant. These factors include abiotic factors such as: through wind or the motion of water and biotic factors such as an insect.
2. This stage is categorised as the pre-penetration period which includes the germination of the spores of the fungus. Here the fungus spores bind to the host and this is due to signals from the host as well as environmental factors.
3. Stage 3 is the process through which the pathogen itself makes contact with the plant through various fungal mechanisms.
4. Here the fungus begins to infect and invade the plant due to making direct contact to the plant's cells. By this stage, the plant itself begins to show symptoms of infection.
5. Now new spores are being made within the plant's cells as the fungus now undergoes reproduction.
6. Once the spores have matured, the fungus releases its spores in order to infect other hosts.
7. Lastly, the spores undergo a period of dormancy to endure conditions that are not favourable until it makes contact with a potential new host.

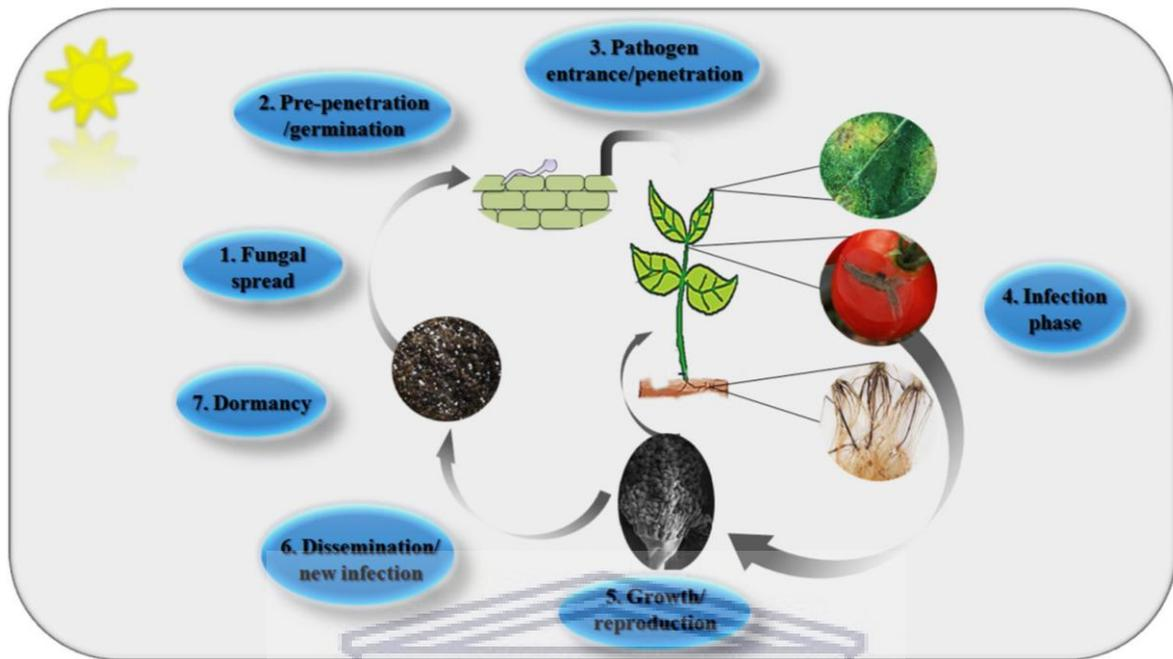


Figure 1.9: Depiction of the disease cycle in plants (Adapted from Zeilinger *et al.*, 2016).

1.8.1 Fusarium species

One of the fungal species that comprises of a very broad genus is the *Fusarium* species. This genus range from mycotoxin producers, phytopathogens and opportunistic human pathogens to microbes that are saprotrophs and biocontrol agents (Summerell *et al.*, 2010). Furthermore this fungal species has a significant role in the agriculture as well as within the economy due to its pathogenicity and ability to produce mycotoxins which affect a large number of plant species (Karlsson *et al.*, 2016; Smith *et al.*, 1988). Examples of *Fusarium* species that are capable of infecting a variety of crops are *F. oxysporum*, *F. solani*, and *F. culmorum*. However infection is dependent on specific environmental conditions and these respective species have been recorded to infect leguminous crops (Šišić *et al.*, 2018). The mycotoxins that are produced by the *Fusarium* species occur during the maturation of the crop itself or in the process of post-harvesting. This is however subsequently determined due to environmental factors. Therefore it is crucial to prevent contamination during the pre-harvest period of the crop species (Niderkorn *et al.* 2006). An ideal candidate for pre-

harvesting treatment would include NPs with wide spread antimicrobial properties (Alaqad and Saleh, 2016).

1.8.1.1 *Fusarium oxysporum*

A study conducted by Sharma *et al.* (2017) confirmed the antimycotic effects of pure cobalt and nickel ferrite for *in vitro* and *in vivo* for three types of pathogenic fungi including *Fusarium oxysporum*, *Colletotrichum gloeosporioides* and *Dematophora necatrix*. Within Molecular Plant Pathology, *Fusarium oxysporum* is ranked as one of the top ten pathogens (Dean *et al.*, 2012). This species can be defined by its ubiquitous nature, that is soil-borne and how it affects plant species through causing vascular wilt (Vlaardingerbroek *et al.*, 2016). When identifying this species on agar media, it can be seen to be either: floccose, sparse or in abundance. Visually its colour is seen to be white, and the species is also cable of producing a magenta pigment (Leslie and Summerell, 2006). The microscopic view of the macro- and microconidia is shown in Figure 1.10. This species is capable of producing mycotoxins, which is known to be detrimental to animals and humans. The mycotoxins are zearalenone, fumonisins as well as a class of trichothecenes. Examples of these trichothecenes are deoxynivalenol, nivalenol and lastly T-2toxin (Niderkorn *et al.*, 2006). Furthermore, the production of the toxins has been suggested to be due to epigenetic modifications that occur within the species (Huang *et al.*, 2019).

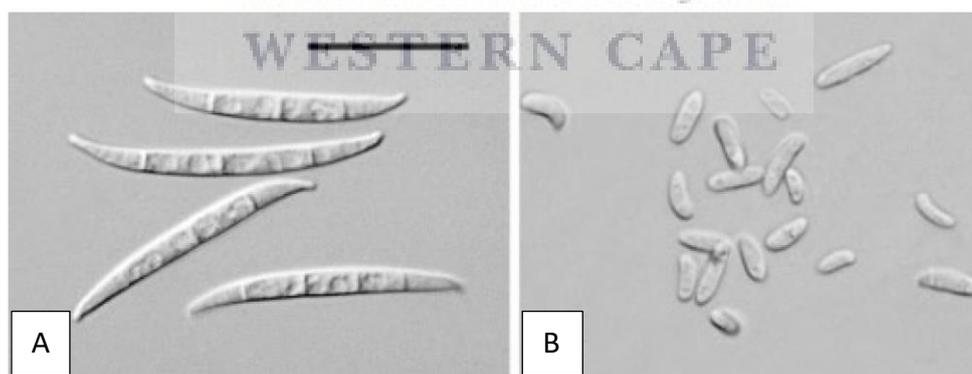


Figure 1.10: An adapted image of *Fusarium oxysporum*, A) Macroconidia and B) Microconidia. Scale Bar: 25 μ m (Leslie and Summerell, 2006).

1.9 Farm maintenance

When addressing crop loss, there are both a qualitative and quantitative factor that contributes to loss of crop yield, whereby quantitative crop loss can be ascribed to detrimental organisms and examples of this is pests, that can either be animals, pathogenic microbes as well as weeds (Savary *et al.*, 2018). Postharvest loss in the farming industry pertains to food loss that occurs throughout the food supply chain from the initial point of harvesting to the consumer consuming the food product (Aulakh *et al.*, 2013). This loss can further be defined as the weight that is being lost due to spoilage, qualitative losses as well as through nutritional loss (Boxall, 2001). Investigating crop loss is considered to be a vital component of a pest management strategy (Youm and Owusu, 1998).

Moretti (2017) states that $\pm 25\%$ of the food and feed outputs on a global scale is seen to be contaminated by mycotoxins. This is in accordance with a Food and Agricultural Organization (FAO) study whereby it was found that *Fusarium* mycotoxins are considered to be economically fundamental when concerning fungal toxins. When addressing farming in South Africa, both biotic and abiotic factors contribute to the farm yield (Beukes *et al.*, 2017). The authors further reported that within South Africa, 25 - 33 % of gross agricultural production is allocated specifically towards grain crops. Furthermore, 33 mycotoxigenic *Fusarium* species are linked to local grain crops, of which *F. oxysporum* has been recorded to infect barley, maize, sorghum and wheat. Whereby the infection caused by *Fusarium* species not only reduces the yield of the crops, but also through the quality of the grains.

1.10 Research Proposal

1.10.1 Problem statement

Fungal diversity is crucial for the ecosystem as well as detrimental to other life forms. *F. oxysporum* is a toxigenic plant pathogen that negatively affect the yield and quality of economically important food/feed crops. This pathogen is an avid mycotoxin producer that presents serious health-related risks/complications for the end user/consumers. Controlling this toxigenic/disease causing pathogen is paramount and although commercialised treatments (pesticides) exists there is a need to explore safer alternatives that will not negatively affect the environment. The use of plant-derived NPs with antimicrobial activity serves as good candidates.

1.10.2 Aims

The aim of this study is to synthesis gold and silver nanoparticles from *Salvia hispanica* leaf extracts and evaluate the antimicrobial activity against *Fusarium oxysporum*.

1.10.3 Objectives of the study

- To optimally synthesise gold and silver nanoparticles from the leaf extract of *Salvia hispanica* -L plants using a biogenic approach.
- To characterise the synthesised gold and silver nanoparticles using:
 - UV-vis spectroscopy (UV-vis),
 - Dynamic light scattering (DLS) analysis,
 - High-resolution transmission electron microscopy (HRTEM),
- To evaluate the antifungal activity of plant-mediated nanoparticles against *Fusarium oxysporum*.



2 Chapter II: Material and methods

2.1 Reagents and suppliers

Table 2.1: List of Reagents used in the investigation

Chemicals	Suppliers
Ca(NO ₃) .4H ₂ O	Sigma-Aldrich
Carbendazim	Sigma-Aldrich
Ethanol 99.9% (EtOH)	Sigma-Aldrich
FeCl ₃	Sigma-Aldrich
Glucose	Sigma-Aldrich
Glycerol	Sigma-Aldrich
Iodine	Sigma-Aldrich
KH ₂ PO ₄	Sigma-Aldrich
MnSO ₄	Sigma-Aldrich
Silver nitrate (AgNO ₃)	Sigma-Aldrich
Tetra chloroauric gold (HAuCl ₄)	Sigma-Aldrich

2.2 Equipment and service providers

Table 2.2: Laboratory equipment used

Equipment	Supplier	Function
Allegra® X-12R	Beckman Coulter, Cape Town, South Africa	Centrifugation of plant extract
FreeZone Plus 2.5L Freeze dryer	Labconco, Kansas City, MO, USA	The crystallisation of plant extract
Incubator OH-800D	Already Enterprise Inc.	Synthesis of AgNPs and AuNPs
Incubator	-	Fungal growth and inhibition testing
Optima Blender	Mellerware	Blend plant extract
POLARstar Omega microplate reader	BMG Labtech, Cape Town, South Africa	UV-Vis spectra
Malvern Zeta sizer	Malvern Instruments Ltd., Malvern, UK	Hydrodynamic size distribution, polydispersity index
TEM Tecnai G2 F20 X-Twin MAT 200 kV Field Emission	FEI Company, USA	Core size distribution, morphology and crystallinity of AgNPs and AuNPs

2.3 Stock solutions and media

Table 2.3: Constituents and stock solutions used

Stock solutions and media	Components
Carbendazim	30 mg in 100 ml EtOH
Glycerol	20 % v/v in dH ₂ O
Potato glucose agar (PGA)	39 g in 1 L dH ₂ O
Silver nitrate	3 mM AgNO ₃ in dH ₂ O, foil wrapped and stored at 4 °C
Tetra chloroauric gold	1 mM HAuCl ₄ in dH ₂ O, foil wrapped and stored at 4 °C

2.4 Nanoparticle synthesis and analysis

2.4.1 Synthesis of green nanoparticles by *Salvia Hispanica*

Salvia hispanica plant extract (40 g) was homogenised in 400 ml (1:10) of boiling water and stirred (Mittal *et al.*, 2013). The sample was separated into 30 ml aliquots for centrifugation. After centrifugation, the supernatant of the samples was passed through Whatman filter paper and freeze-dried for 5 days (Figure 2.1). The extracts consisted of 0.125 - 32 mg/ml of plant extract dissolved in dH₂O. Furthermore, silver nitrate was made up to a concentration of 3 mM with dH₂O and tetrachloroauric gold was made up to 1 mM in dH₂O. The plant extract was added to silver nitrate or tetra chloroauric gold solution in 1:5 v/v and heated at 25 and 70 °C respectively while shaking at 400 rpm.

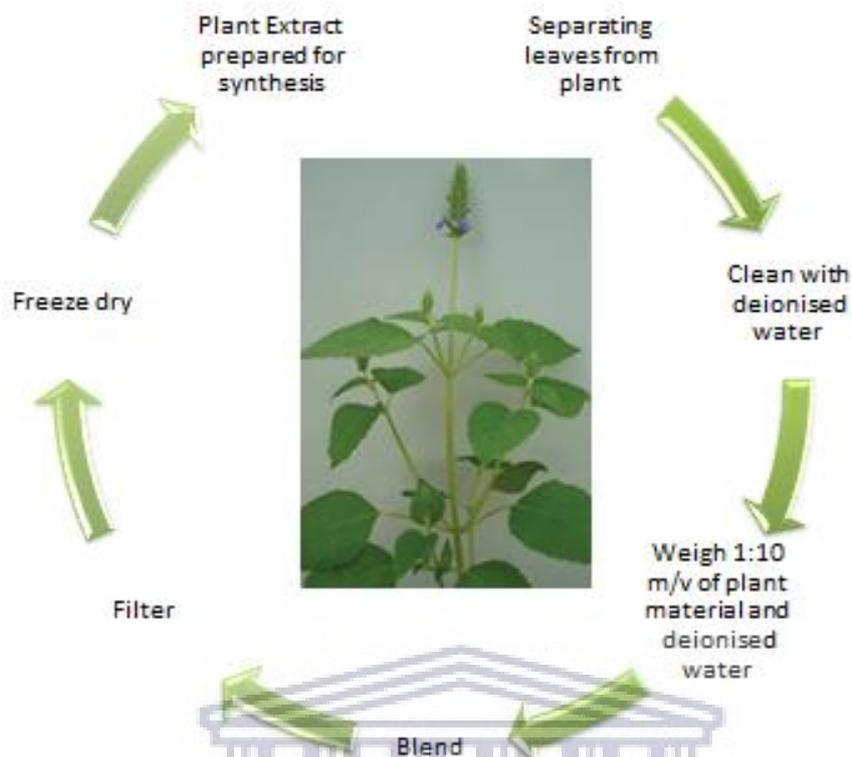


Figure 2.1: Preparation of Plant-extract material. The image of the *Salvia hispanica* plant was received (Adapted from Mohd Ali *et al.*, 2012).

2.4.2 UV-vis analysis

In 96-well microtiter plates, aliquots of each synthesised NPs were added at a volume of 1:3 v/v ratio of NP solution and dH₂O in separate wells respectively. Spectrum analysis was then done via UV-vis across the wells on a nanometre range to assess for the success of NPs being synthesised. The frequency range for AgNp was from 300-600 nm whereas AuNPs were screened from 350-750 nm. The aliquot order went from a blank, which was dH₂O, followed by 3mM silver nitrate, then the NPs solutions 0.125- 32 mg/ml of plant extract. The same was done for the Au synthesis. This was done for reactions that occurred at 25°C as well as 70 °C.

2.4.3 Dynamic light scattering

Aliquots of the synthesised NPs was then placed into quartz cuvette and analysed by the Malvern Zeta sizer for its hydrodynamic size of the NPs as well as for its polydispersity index- which is to determine the uniformity of the NPs. The samples that were analysed were based on the UV-vis data (section 2.4.2).

2.4.4 High-Resolution Transmission Electron Microscopy analysis

To determine the core morphology of the Au- and AgNPs, the samples were prepared via drop-coating one drop of the solution onto a carbon-coated copper grid. The sample was then dried under a Xenon lamp for 10 minutes and analysed with HRTEM with the conditions being set in brightfield mode at an accelerating voltage of 200 kV.

2.5 Antifungal testing

2.5.1 Evaluation of antifungal activity from plant and plant mediated NPs

Antifungal activities of plant extracts and plant-mediated NPs were evaluated using well diffusion method on potato glucose agar (PGA). Carbendazim at different concentrations (0.1, 0.2, 0.3 mg/ml) was used as control against *F. oxysporum*. An ethanol control was also included to ensure antifungal activity was not influenced by ethanol (carbendazim dissolved in ethanol). For each PGA plate, four wells (diameter = 6 mm) at opposite ends of the petri dish were prepared using a sterile cork borer. The assay was used to evaluate the inhibition of fungal growth using the freshly synthesised AgNPs and plant extracts. For each petri dish used in this study, a freshly maintained 1 cm x 1 cm *F. oxysporum* agar plug was aseptically transferred to the middle of the PGA plate surrounded by the four wells. For the carbendazim control, each well was filled with 100 µl of carbendazim at different concentrations. To measure the antifungal activity of each plant extract, 100 µl of each extract was added to each well. To measure antifungal activity of the AgNPs synthesised from three different plant extracts, two wells each were filled with 100 µl AgNPs at a final concentration of 4 mg/ml whereas the other two wells were filled with 100 µl of AgNPs at a final concentration of 10 mg/ml. All plates were in an incubator at 30 °C for 7 days.

3 Chapter III: Biogenic synthesis and characterisation of gold and silver nanoparticles from *Salvia hispanica* L. leaf extracts

3.1 Introduction

When discussing synthesis routes for making nanomaterial, there are three main pathways: Physical, chemical and biological. Furthermore, this synthetic route is also known as biogenic or green synthesis and is considered a bottom route for making NPs from organic matter (Alaqad and Saleh, 2016). Whereby nanomaterial occur within 1D to 3D of which 1D NPs are recorded to be <100 nm in size and usually take on the shape of being spherical (Delgado-Ramos, 2014). The use of green synthesis has been noted to be a simple protocol that can be achieved through one step and is seen to be cost-effective. Moreover, the protocol itself is reproducible of which the material being used is regarded to be stable (Mittal *et al.*, 2013). Another reason for wanting to synthesis NPs from plant matter is because the material contains both the reducing and stabilising agent that is needed for metal NPs synthesis (Kumar and Yadav, 2009).

Of the *Lamiaceae* family, the largest genus to come from the family makes up approximately 1000 various species known as the *Salvia* plant. The plant's name stems from the Latin word: *salvare* that is translated to mean: healing properties (Topçu, 2006). The plant's origins are specific to South Africa, Central and South America, Asia and also the Mediterranean regions. *Salvia hispanica* is a plant species that is cultivated biannually and is recognised for its active ingredients such as its essential fatty acids. It is indigenous to South America and is renowned for its medicinal uses. Furthermore, this is where the species received its common name from Chia (Jamboonsri *et al.*, 2012). The phytochemicals that can be found within Chia have been identified to have changeability in concentration due to the respective conditions in which the species can be found cultivated in. These conditions include farming conditions, temperature, and the accessibility of nutrients (Mohd Ali *et al.*, 2012).

The aim of this study is to synthesis and characterise Au- and AgNPs. The synthesised NPs will be quantitatively and qualitatively characterised using UV-vis, DLS, and HRTEM.

3.2 Results and Discussion

3.2.1 Synthesis and characterisation

Before undergoing the characterisation of the nanomaterial, visual confirmation was also conducted. This means that a visual assessment was done to confirm that there was a chemical reaction that had occurred simply by observing a colour change. AgNPs appear to be brown/orange (Figure 3.1) (Ahmed *et al.*, 2016; Alaqad and Saleh, 2016) whereas AuNPs appears as red/purple (Alaqad & Saleh, 2016). This colour change is the first indication of a chemical reaction and is an indirect confirmation step used prior to subsequent characterisations.

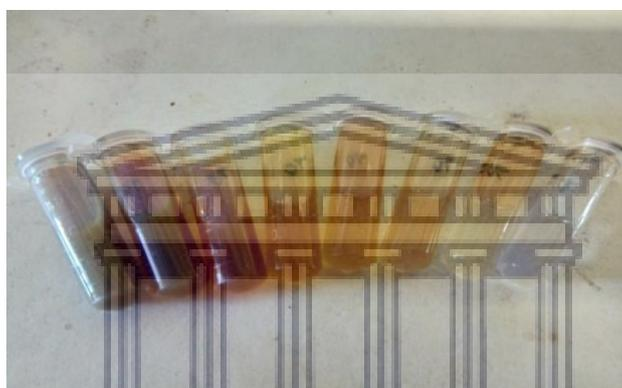


Figure 3.1: Visual representation of the colour changes associated with AgNP formation across a plant extract concentration gradient

3.2.2 UV-vis spectrometry

The use of UV-vis for the sake of characterisation is for identification, confirmation as well as the initial check of uniformity (Alaqad and Saleh, 2016). This means that because each nanomaterial i.e., Au- or AgNP have their specific plasmon resonance. The material will be identified and confirmed through UV-vis through a peak in the graph. Moreover, the shape and bend of the curve can be seen as the preliminary confirmation of uniformity (Alaqad and Saleh, 2016). After synthesising NPs for an hour at 70 °c and 25 °c respectively for the plant extract concentrations of 16 mg/ml - 0.125 mg/ml.

3.2.2.1 *Leaf extract for silver nanoparticles(AgNPs)*

When using UV-vis for AgNPs a peak is expected to occur around 410 nm (Alaqad and Saleh, 2016). When screening the synthesis of leaf extract at 25 °C it was found that synthesis was

successful for 0.25 - 2 mg/ml of plant extract (Figure 3.2A) where the greatest peak formed most significantly for 2 mg/ml. There was no synthesis for 8 - 32 mg/ml plant extract. When compared to the 70 °C syntheses occurred for 0.125 - 2 mg/ml of leaf extract (Figure 3.2B) whereby 2 mg/ml again was the reaction that had the most pronounced peak, resulting in a greater peak when compared to the 25 °C reactions. The synthesis was unsuccessful for 4 - 16 mg/ml plant extracts. When comparing the peaks of the two temperatures. Furthermore a λ max of 444 nm at 25 °C it was observed to have an absorbance of 0.879 au and λ max was 432 nm at 70 °C with an absorbance of 1.228 au. This was indicative of a greater product yield at 70 °C for the plant extract of 2 mg/ml which was the highest peak for both respective temperatures.

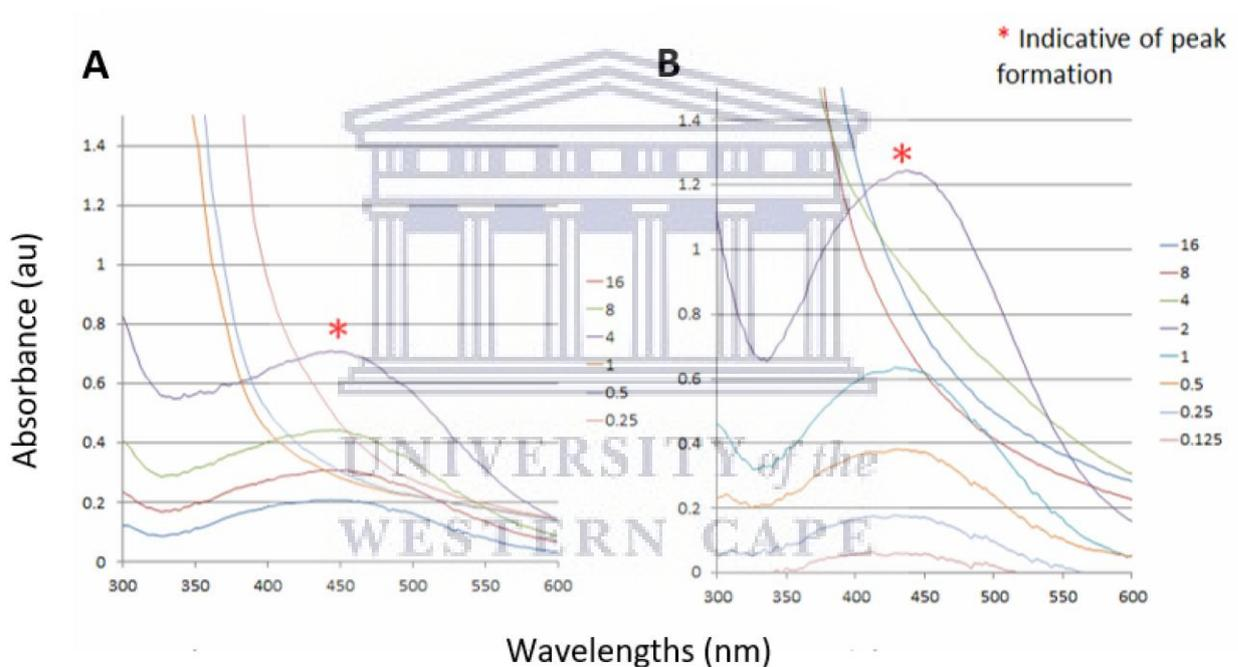


Figure 3.2: UV-vis of silver nanoparticles at various plant extract concentrations. Nanoparticles were synthesised at 25 °C (A) and 70 °C (B) respectively. AgNPs synthesis from leaf extracts at different concentrations (A-B).

3.2.2.2 Leaf extract for gold nanoparticles (AuNPs)

When using UV-vis for AuNPs a peak is expected to occur around 550 nm (Elbagory *et al.*, 2016; Alaqad and Saleh, 2016). When screening the synthesis of leaf extract at 25 °C it was found that synthesis was successful for 16- and 32 mg/ml of leaf extract (Figure 3.3A) and was unsuccessful for 0.25 - 8 mg/ml. Whereby 32 mg/ml was found to have the most

pronounced peak for synthesis. When looking at the reaction that occurred at 70 °C, synthesis was successful for leaf extract concentrations ranging from 4 - 32 mg/ml (Figure 3.3B) with 32 mg/ml still being the most pronounced peak, even more so than when synthesised at 25 °C. The reaction did not occur for extract concentrations of 0.125 - 2 mg/ml. Furthermore λ max of 538 nm at 25 °C it was observed to have an absorbance of 1.902 au and λ max was 538 nm at 70 °C as well with an absorbance of 3.136 au which was indicative of a greater product yield was at 70 °C for the plant extract of 32 mg/ml which was the highest peak for both respective temperatures.

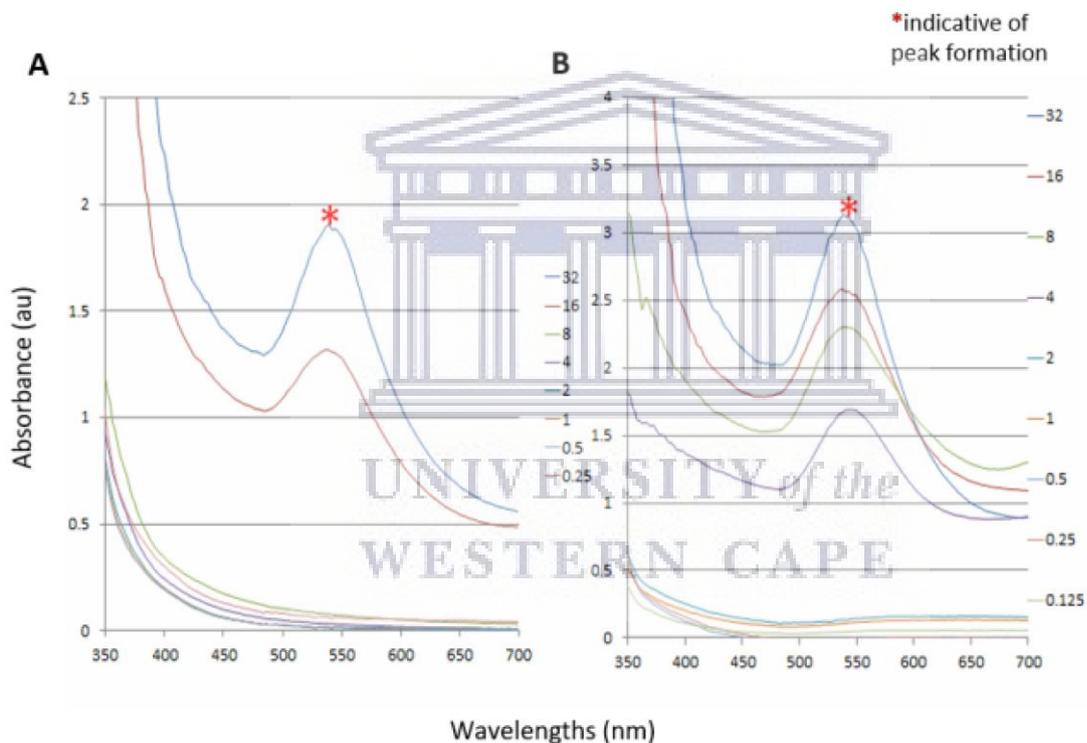


Figure 3.3: UV-Vis of gold nanoparticles at various plant extract concentrations. Nanoparticles were synthesised at 25 °C (A) and 70 °C (B) respectively. AuNPs synthesis from leaf extracts at different concentrations (A-B).

3.2.3 Dynamic Light scattering (DLS)

DLS is a characterisation tool used that is often coupled with other characterisation techniques such as UV-Vis and TEM. This is because the function of DLS to determine the particle size of NPs whilst suspended in liquid media (Hoo *et al.*, 2008). The NPs are analysed

as the light gets scattered off from them which then results in localised variations within the refractive index of the solution (Hoo *et al.*, 2008). In doing so this tool determines the hydrodynamic size of the NPs.

After an hour synthesis reaction of NPs and based on the UV-vis data the leaf extract concentrations of 2, 1 mg/ml at 25 °C and 2, 1, and 0.5 mg/ml at 70 °C samples for the AgNPs and 32 and 16 mg/ml at 25 °C and 32, 16, and 8 mg/ml at 70 °C of leaf extract for AuNPs were taken for DLS analysis (Table 3.1). The hydrodynamic size was determined by scanning the sample 7 times and the process was repeated for 3 repeats, after which an average size was determined. The pdi is present to confirm the uniformity of the particles which were all below 0.5 which is an indication of mono-dispersity within the samples. Therefore the samples that were synthesised at 25 °C and 70 °C all reported being uniform in size based on their pdi. The uniformity of the NPs was also less than 0.4 based on their respective pdi which validates that the samples were unimodal.

Table 3.1: Dynamic light analysis of gold and silver Nanoparticles. Which is the average size of the silver and gold nanoparticles.

Concentration (mg/ml)	Plant region	Metal	Temperature (°C)	Z-average	Polydispersive index (PDI)
2	Leaf	Silver	25	87.22	0.376
1	Leaf	Silver	25	56.16	0.357
2	Leaf	Silver	70	83.99	0.351
1	Leaf	Silver	70	104.0	0.344
0.5	Leaf	Silver	70	42.28	0.282
32	Leaf	Gold	25	77.50	0.354
16	Leaf	Gold	25	66.11	0.392
32	Leaf	Gold	70	164.6	0.334

16	Leaf	Gold	70	188.6	0.391
8	Leaf	Gold	70	175.5	0.334

3.2.4 Transmission Electron Microscopy (TEM) analysis

Alaqad and Saleh (2016) recorded that the functions of TEM are for morphology, shape as well as particle size. This is because TEM is a visual tool used to see the NPs to scale.

The NPs that were synthesised with 2 mg/ml of plant extract regarding AgNPs synthesis, as well as 32 mg/ml of plant extract for AuNPs, were observed under HRTEM to determine visually the morphology of the nanoparticles as well as to identify their shape and size. The nanoparticles were viewed at the following magnification: 50 nm and 2 nm (Figure 3.4 and 3.5).

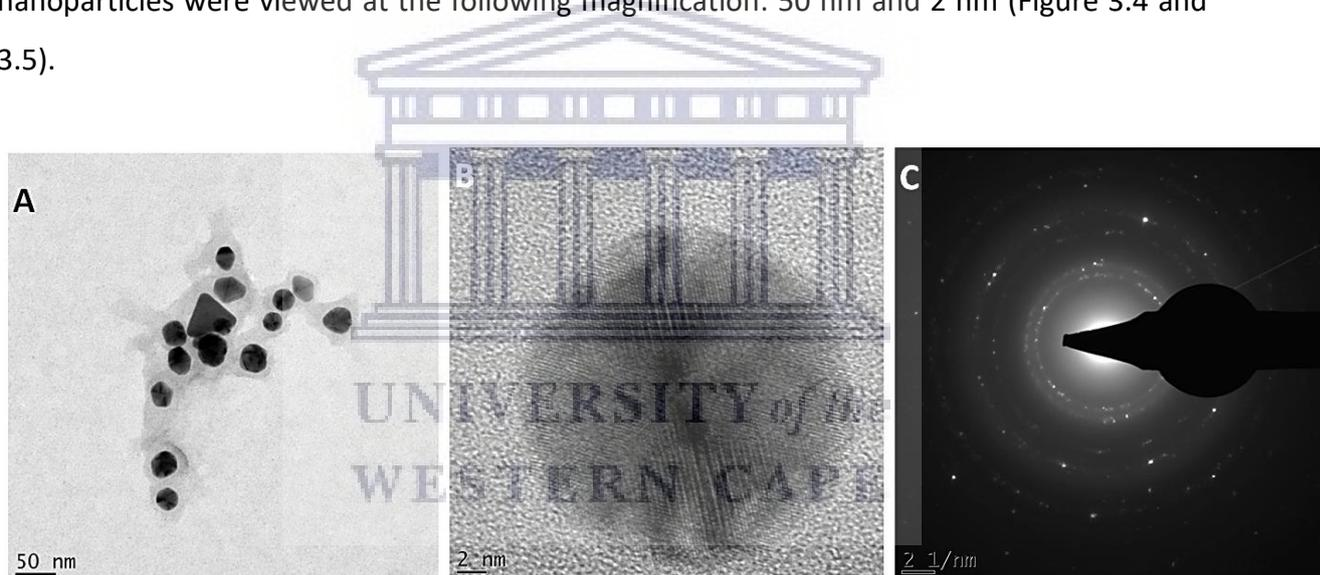


Figure 3.4: Transmission Electron Microscopy for silver nanoparticles. A) Silver Nanoparticles that were viewed 50 nm as per the scale depicted by the scale bar in the bottom left. This depicts uniformity in the size of the nanoparticles however non-uniform in shape. B) This displays the crystallinity at 2 nm as depicted by the scale bar in the bottom left corner. C) This is the SAED patterns that depict the diffraction rings of FCC Ag.

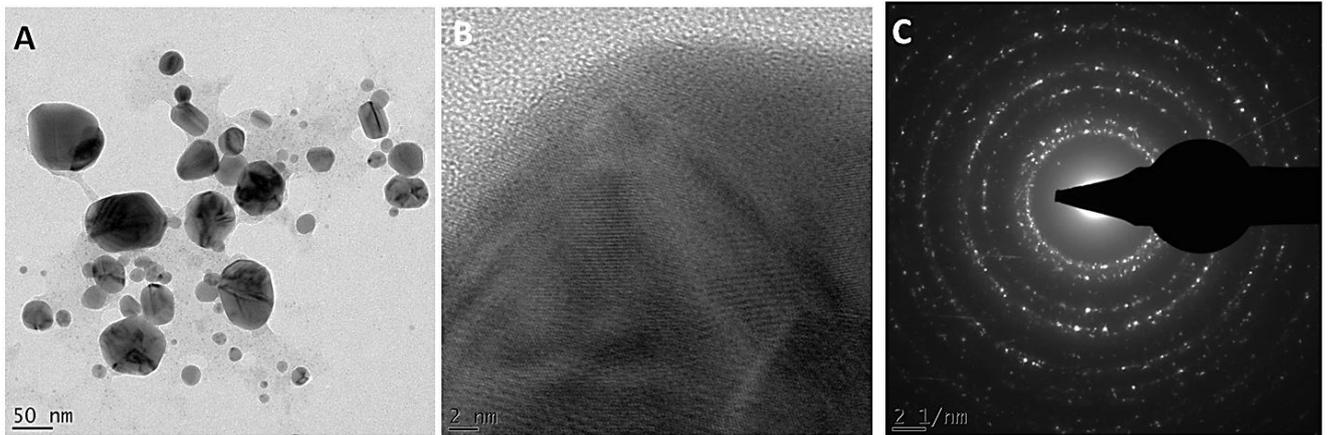


Figure 3.5: Transmission Electron Microscopy for gold nanoparticles. A) Gold Nanoparticles that were viewed 50 nm as per the scale depicted by the scale bar in the bottom left. This depicts uniformity in the size of the nanoparticles however non-uniform in shape. B) This displays the crystallinity at 2 nm as depicted by the scale bar in the bottom left corner. C) This is the SAED patterns that depict the diffraction rings of FCC Au.

Whereby the shape of the NPs is not conforming to one shape however they are unimodal in size. This suggests possibly more than one phytochemical being responsible for NP synthesis as well as the abundance of the respective phytochemicals. In Figure 3.4C and 3.5C, the selected area electron diffraction (SAED) patterns of the NPs are being depicted with their diffraction rings index that conferred to the face-centred cubic (FCC) Ag and Au respectively. The SAED patterns of the NPs are further confirmation of the respective metals as they depict with their diffraction rings index that confers to the FCC Ag and Au crystals respectively (Joe *et al.*, 2017; Elbagory *et al.*, 2016).

4 Chapter IV: Antifungal activities of plant extracts and plant-mediated silver nanoparticles

4.1 Introduction

The role of Fungi in the ecosystem and modern agriculture has become pivotal due to their nutritional versatility and its effect on plants. They are regarded as important decomposers and organic recyclers of organic matter. However, Fungi serve dual roles in nature by being either beneficial or detrimental to the roots and atypical regions of various plant species (Zeilinger *et al.*, 2016; Horwitz *et al.*, 2013). Majority of plant relationships are seen to either be symbiotic or neutral - with parasitic infections being an exception - henceforth plants are considered to resistant to a wide range of pathogens (Staskawicz, 2001). Furthermore, the plant's health is dependent on the type of microbial activity found within the rhizosphere and the microbes that work directly in the plant (Zeilinger *et al.*, 2016). When looking at the type of infections that occur within plant species, it has been seen that 70-80 % of their diseases are due to fungal infections which can occur from 10 000 different fungal species that are considered to be plant pathogen (Agrios, 2005).

The genus: *Fusarium* comprises of a broad number of fungal species. These organisms range from being mycotoxin producers, phytopathogens to saprotrophs and biocontrol agents (Summerell *et al.*, 2010). *Fusarium* plays a crucial role in the agricultural- and economic sector because of its pathogenicity and its capability of producing mycotoxins that can affect a large number of plant species (Smith *et al.*, 1988; Karlsson *et al.*, 2016). One of the top ten ranked plant pathogens by Molecular Plant Pathology is *Fusarium oxysporum*, a ubiquitous organism noted to be soil-borne that affects plant species by producing vascular wilt (Vlaardingerbroek *et al.*, 2016; Dean *et al.*, 2012).

The aim of this chapter is to evaluate the antifungal activity of plant extracts *Salvia hispanica*, *Salvia Africana-L* and *Cotyledon orbiculata L.* and plant derived AgNPs against *Fusarium oxysporum*.

4.2 Results and Discussion

4.2.1 Positive control (Carbendazim) against *Fusarium oxysporum*

For this section of research, a positive control was required. This meant that a known fungicide was required to confirm inhibition of *Fusarium oxysporum* a soil-borne plant pathogen that infects plants (Vlaardingerbroek *et al.*, 2016; Dean *et al.*, 2012). In a study conducted by Wani *et al.* (2011) many fungicides were tested for inhibitory properties against *Fusarium oxysporum*. One of the fungicides was carbendazim, a commercial antifungal agent. Zhang *et al.* (2018) further went onto test the solubility of carbendazim in organic solvents namely alcohols due to carbendazim having poor solubility within H₂O. Therefore for this study carbendazim was dissolved in EtOH. An EtOH was included to ensure that the EtOH does not contribute to the influence of antifungal activity observed in the carbendazim treatment.

A well-diffusion assay was performed using carbendazim at different concentrations (0.1-, 0.2-, and 0.3 mg/ml) as positive control to quantitatively measure, the level of inhibition as observed for mycelial growth. After 7 days of incubation at 30 °C, *F. oxysporum* mycelial growth was measured at 55 mm. The results showed that the mycelial growth of *F. oxysporum* was restricted in a concentration dependent manner with the higher concentrations showing the greatest level of growth inhibition. In response to carbendazim at a final concentration of 0.1 mg/ml the mycelial growth was restricted to 45 mm whereas 0.2 mg/ml and 0.3 mg/ml completely suppressed mycelial growth when compared to the control (Figure 4.1).

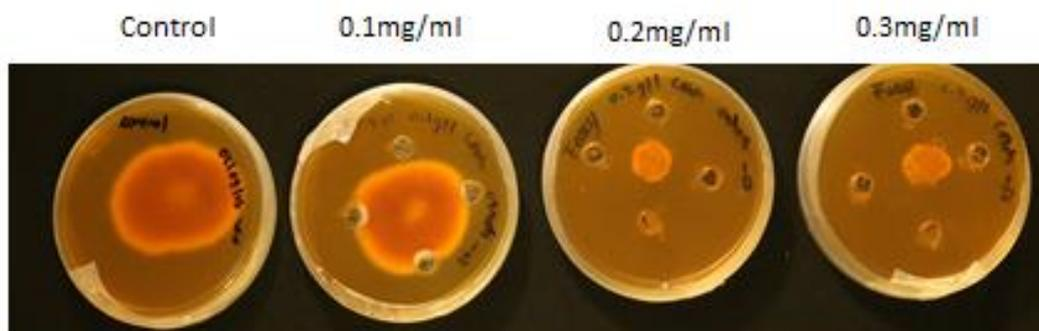


Figure 4.1: Antifungal activity of carbendazim against *F. oxysporum*. Mycelial growth was restricted in a concentration dependent manner. Carbendazim at 0.1 mg/ml restricted mycelial growth to 45 mm whereas 0.2 mg/ml and 0.3 mg/ml completely inhibited mycelial growth on PGA plates after 7 days at 30 °C.

4.2.2 Antifungal activity of plant extracts

In a study by Nkomo *et al.* (2014), he showed that plant extracts have antifungal properties and goes on to mention that Minimum inhibitory concentration (MIC) for these extracts to be considered for strong inhibition needs to be ≤ 0.5 mg/ml. He then goes on to say that inhibition that occurs above 1.6 mg/ml is considered weak. When the leaf extracts from *Cotyledon orbiculata var. oblonga*, *Salvia Africana-lutea* and *Salvia hispanica* were tested against *F. oxysporum* no significant inhibition of mycelial growth was observed. This could be due to the method of testing and possibly exploring the spread plate technique instead of the well-diffusion assays. Well-diffusion was chosen due to the quantity of product being greater, however poor diffusion through the wells may have been a factor. The well-diffusion was performed on plant extract: *Salvia Africana-lutea*, *Cotyledon orbiculata var. oblonga* and *Salvia hispanica* at 10 mg/ml and 4 mg/ml and aliquoted at a volume of 100 μ l in each well and was incubated for 7 days however there was no significant difference in the growth of the control and the respective plant extract concentrations (Figure 4.2). The control mycelial growth was measured at 70 mm with no significant growth inhibition observed for each plant extracts.

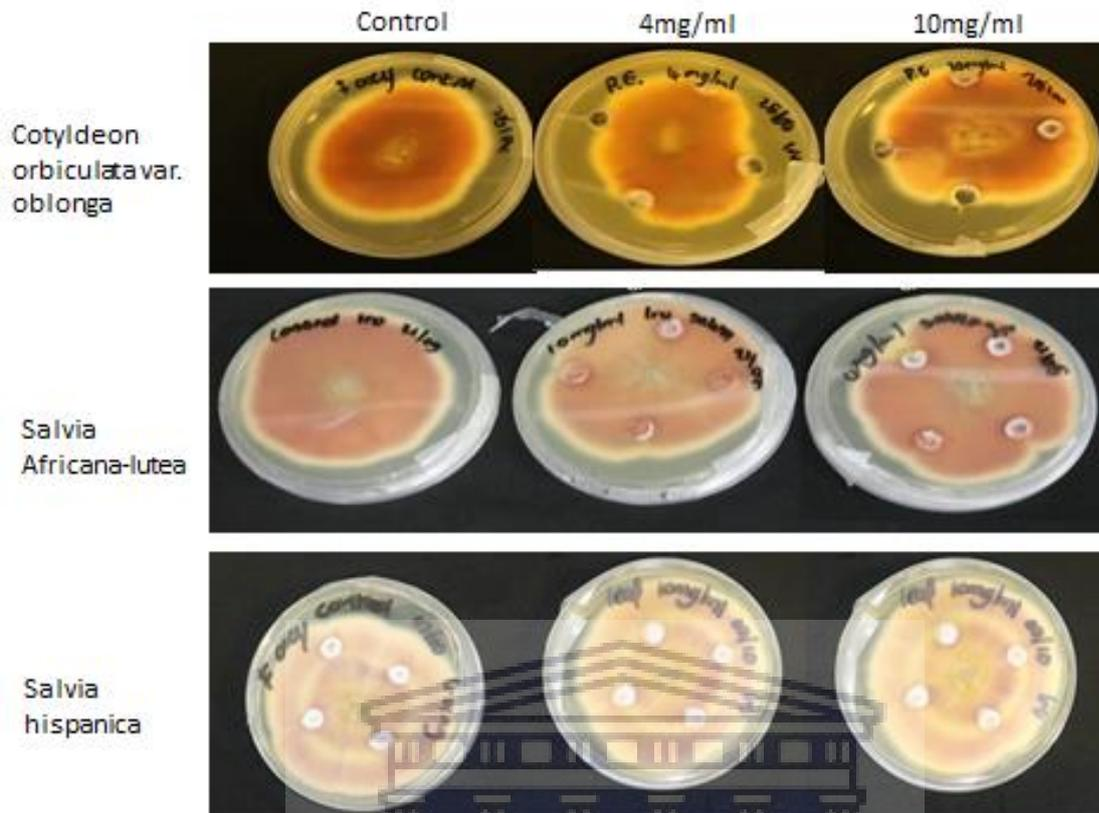


Figure 4.2: Antifungal activity of *Cotyledon orbiculata var. oblonga* extract, *Salvia Africana-lutea* extract and *Salvia hispanica* extracts against *F. oxysporum*. No changes in mycelial growth were observed in response to different concentration (4 mg/ml and 10 mg/ml) of plant extract. All samples incubated for 7 days at 30 °C

UNIVERSITY of the
WESTERN CAPE

4.2.3 Antifungal activity of plant derived AgNPs

In table 1.1 Kaur *et al.* (2018) and Kim *et al.* (2012) conducted antifungal testing against fungi for AgNPs which showed promise for this component of research. An antifungal well-diffusion assay was performed using AgNPs synthesised from three plant species namely *Salvia africana-lutea*, *Cotyledon orbiculata var. oblonga*, and *Salvia hispanica* (Figure 4.3)

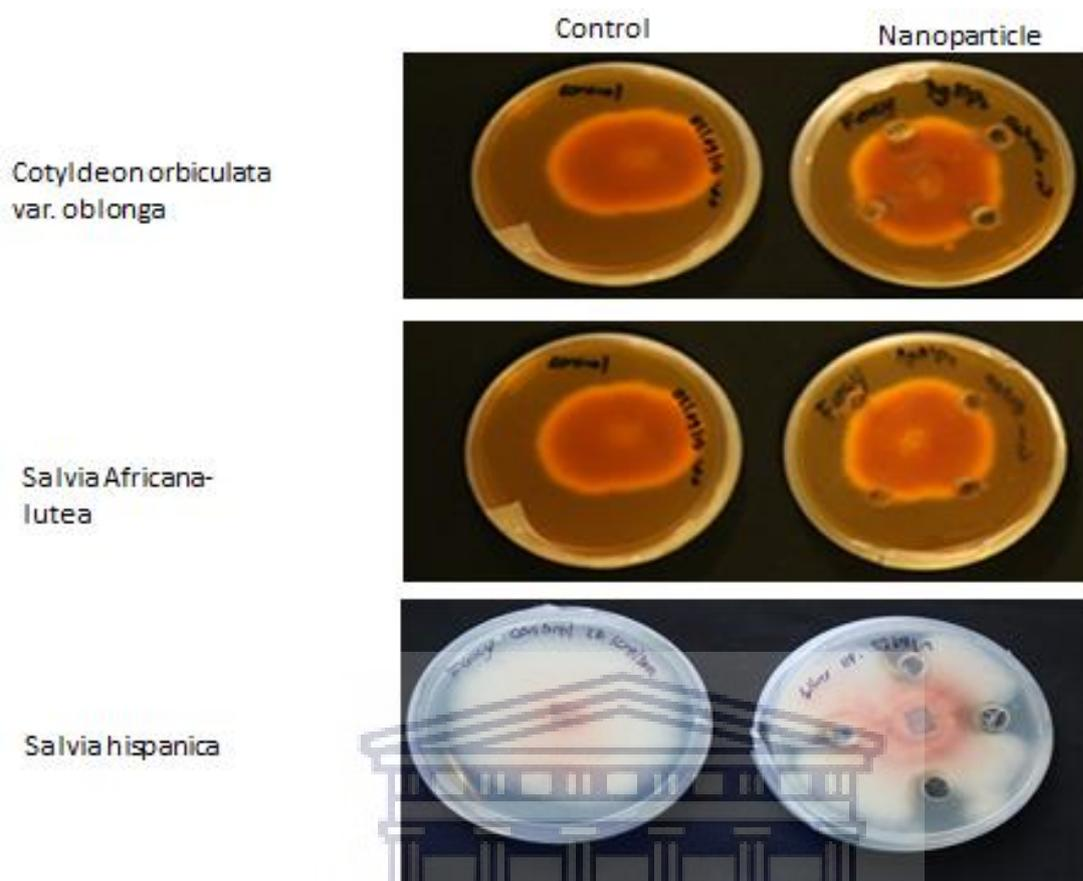


Figure 4.3: Well diffusion antiungal activity assay of *Cotyledon orbiculata var. oblonga*, *Salvia Africana-lutea* and *Salvia hispanica L.* derived AgNPs against *F. oxysporum*. The fungus was allowed to grow for 7 days at 30 °C. No significant reduction in mycelial growth was measured in response to AgNPs from *Cotyledon orbiculata var. oblonga* and *Salvia Africana-lutea*. Fungal mycelial growth reduction was observed in response to AgNPs synthesised from *Salvia hispanica L.*

The results showed that no antifungal activity (as seen as restrictive mycelial growth) was observed for AgNPs derived from *Salvia africana-lutea* and *Cotyledon orbiculata var. oblonga*. Relative to their respective controls, no change in *F. oxysporum* mycelial growth was observed. Interestingly, a distinct clear zone around the wells was observed in response to AgNPs synthesised from *Salvia hispanica* extracts. The zone of clearance around the wells was measured at 10 mm in diameter, which suggest that AgNPs derived from *Salvia hispanica* do have antifungal activity. To our knowledge, this was the first attempt to measure antifungal activity from AgNPs synthesised from *Salvia hispanica*. The work presented here lays the foundation for a more elaborative study on NP synthesis from this plant species to explore the antimicrobial activity possessed by these remarkable nano-species. The lack of antifungal activity observed from *Salvia Africana-lutea* and *Cotyledon orbiculata var. oblonga* could be ascribed to the antifungal activity assay or perhaps the methods used to synthesise NPs.

5 Chapter V: Conclusion and future work

5.1 Synthesis of gold and silver nanoparticles from *Salvia hispanica*

Using plant extract from *Salvia hispanica* for the synthesis of Au- and AgNPs has proven to be successful based on the UV-vis spectroscopy for the leaf extract. Furthermore, based on UV-vis and DLS data the NPs that were formed were uniform in their size range. TEM imagery further specified the formation of the NPs that were not confined to a specific shape. Furthermore, they conformed to their SAED pattern in regards to FCC Ag and Au respectively.

5.2 Antifungal activity against *Fusarium oxysporum*

Upon antifungal screening via well-diffusion of carbendazim it was proven to inhibit the mycelial growth of the fungus at the concentrations: 0.2 and 0.3 mg/ml respectively when compared to the control. When testing the antifungal activity of the AgNPs it was found that via well-diffusion the fungus' growth was not inhibited for AgNPs that were synthesised from *Salvia africana-lutea* and *Cotyledon orbiculata* var. *oblonga*, however, the NPs that were synthesised from *Salvia hispanica* was found to be successful for inhibition and displayed a zone of clearance. The plant extract from which NPs were synthesised also seemed to not be able to inhibit the mycelial growth of the fungus.

5.3 Future works

5.3.1 Nanoparticle analysis

Further NP characterisation that could be done on both the Au- and AgNPs that were synthesised from the *Salvia hispanica* could be Fourier-Transform Infrared analysis to determine possible functional groups involved in the bonding of the NPs in comparison to that with the plant extract (Alaqad and Saleh, 2016). Furthermore, the zeta-potential could be investigated in order to determine the charge of the NPs for further characterisation of the NPs. Moreover, identifying the stability of the nanoparticles in media other than that of water could also be tested.

5.3.2 Antifungal activity

The antifungal activity of plant extract and plant-derived NPs against *F. oxysporum* could be investigated in liquid cultures. Furthermore, the antifungal activity/biocontrol of *F.*

oxysporum could be tested in plants by priming seeds with plant extract and plant-derived AgNPs and monitor plant growth performances under pathogen infection.



UNIVERSITY *of the*
WESTERN CAPE

Reference List

- Agrios, G. N. (2005) *Plant Pathology*. 5th edn. Amsterdam: Elsevier Academic Press.
- Ahmad, T. *et al.* (2013) 'Antifungal activity of gold nanoparticles prepared by solvothermal method', *Materials Research Bulletin*, 48(1), 12–20.
- Ahmed, S. *et al.* (2016) 'A review on plants extract mediated synthesis of silver nanoparticles for antimicrobial applications: A green expertise', *Journal of Advanced Research*, 7(1), 17–28.
- Alaqad, K. and Saleh, T. A. (2016) 'Gold and Silver Nanoparticles: Synthesis Methods, Characterization Routes and Applications towards Drugs', *Journal of Environmental & Analytical Toxicology*, 6(4).
- Amabeoku, G. J. *et al.* (2001) 'Analgesic and antipyretic effects of *Dodonaea angustifolia* and *Salvia africana-lutea*', *Journal of Ethnopharmacology*, 75(2–3), 117–124.
- Amendola, V. and Meneghetti, M. (2009) 'Size Evaluation of Gold Nanoparticles by UV-vis Spectroscopy', *The Journal of Physical Chemistry C*, 113(11), 4277–4285.
- Aulakh, J. *et al.* (2013) *Estimating Post-Harvest Food Losses: Developing a Consistent Global Estimation Framework*, *AgEcon Search*.
- Beukes, I. *et al.* (2017) 'Mycotoxigenic *Fusarium* species associated with grain crops in South Africa - A review', *South African Journal of Science*, 113(3–4), 1–12.
- Boxall, R. A. (2001) 'Post-harvest losses to insects—a world overview', *International Biodeterioration & Biodegradation*, 48(1–4), 137–152.
- Dean, R. *et al.* (2012) 'The Top 10 fungal pathogens in molecular plant pathology', *Molecular Plant Pathology*, 13(4), 414–430.
- Delgado-Ramos, G. C. (2014) 'Nanotechnology in Mexico: Global trends and national implications for policy and regulatory issues', *Technology in Society*, 37, 4–15.
- Elbagory, A. M. *et al.* (2016) 'Large Scale Screening of Southern African Plant Extracts for the Green Synthesis of Gold Nanoparticles Using Microtitre-Plate Method', *Molecules (Basel, Switzerland)*, 21(11).
- Elbagory, A. M. *et al.* (2017) 'Inhibition of Bacteria Associated with Wound Infection by Biocompatible Green Synthesized Gold Nanoparticles from South African Plant Extracts', *Nanomaterials (Basel, Switzerland)*, 7(12), 417.

Hoo, C. M. *et al.* (2008) 'A comparison of atomic force microscopy (AFM) and dynamic light scattering (DLS) methods to characterize nanoparticle size distributions', *Journal of Nanoparticle Research*, 10(S1), 89–96.

Horwitz, B. A. *et al.* (eds) (2013) *Genomics of Soil- and Plant-Associated Fungi*. Berlin, Heidelberg: Springer Berlin Heidelberg (Soil Biology).

Hu, M. *et al.* (2006) 'Gold nanostructures: engineering their plasmonic properties for biomedical applications', *Chemical Society Reviews*, 35(11), 1084–1094.

Huang, D. *et al.* (2019) 'The epigenetic mechanisms in Fusarium mycotoxins induced toxicities', *Food and Chemical Toxicology: An International Journal Published for the British Industrial Biological Research Association*, 123, 595–601.

Jamboonsri, W. *et al.* (2012) 'Extending the range of an ancient crop, *Salvia hispanica* L.—a new ω 3 source', *Genetic Resources and Crop Evolution*, 59(2), 171–178.

James, T. (1963) 'Use of *Cotyledon orbiculata* L. in treatment of plantar wart (*Verruca plantaris*)', *Archives of Disease in Childhood*, 38, 75–76.

Jayaseelan, C. *et al.* (2013) 'Green synthesis of gold nanoparticles using seed aqueous extract of *Abelmoschus esculentus* and its antifungal activity', *Industrial Crops and Products*, 45, 423–429.

Joe, M.-H. *et al.* (2017) 'Phytosynthesis of Silver and Gold Nanoparticles Using the Hot Water Extract of Mixed Woodchip Powder and Their Antibacterial Efficacy', *Journal of Nanomaterials*, 2017, 1–19.

Kalatehjari, P., Yousefian, M. and Khalilzadeh, M. A. (2015) 'Assessment of antifungal effects of copper nanoparticles on the growth of the fungus *Saprolegnia* sp. on white fish (*Rutilus frisii kutum*) eggs', *The Egyptian Journal of Aquatic Research*, 41(4), 303–306.

Karlsson, I. *et al.* (2016) 'Genus-Specific Primers for Study of *Fusarium* Communities in Field Samples', *Applied and Environmental Microbiology*. Edited by D. Cullen, 82(2), 491–501.

Kaur, T., Kapoor, S. and Kalia, A. (2018) 'Synthesis of Silver Nanoparticles from *Pleurotus florida*, Characterization and Analysis of their Antimicrobial Activity', *International Journal of Current Microbiology and Applied Sciences*, 7(07), 4085–4095.

Kim, S. W. *et al.* (2012) 'Antifungal Effects of Silver Nanoparticles (AgNPs) against Various Plant Pathogenic Fungi', *Mycobiology*, 40(1), 53–58.

Klueh, U. *et al.* (2000) 'Efficacy of silver-coated fabric to prevent bacterial colonization and subsequent device-based biofilm formation', *Journal of Biomedical Materials Research*, 53(6), 621–631.

Kumar, V. and Yadav, S. K. (2009) 'Plant-mediated synthesis of silver and gold nanoparticles and their applications', *Journal of Chemical Technology & Biotechnology*, 84(2), 151–157.

Larue, C. *et al.* (2014) 'Foliar exposure of the crop *Lactuca sativa* to silver nanoparticles: evidence for internalization and changes in Ag speciation', *Journal of Hazardous Materials*, 264, 98–106.

Leslie, J. F. and Summerell, B. A. (eds) (2006) 'Frontmatter', in *The Fusarium Laboratory Manual*. Ames, Iowa, USA: Blackwell Publishing, i–xii.

Mittal, A. K., Chisti, Y. and Banerjee, U. C. (2013) 'Synthesis of metallic nanoparticles using plant extracts', *Biotechnology Advances*, 31(2), 346–356.

Mittal, J. *et al.* (2014) 'Phytofabrication of nanoparticles through plant as nanofactories', *Advances in Natural Sciences: Nanoscience and Nanotechnology*, 5(4), 043002.

Mohd Ali, N. *et al.* (2012) 'The Promising Future of Chia, *Salvia hispanica* L.', *Journal of Biomedicine and Biotechnology*. Edited by K. Husain, 2012, 171956.

Niderkorn, V., Boudra, H. and Morgavi, D. P. (2006) 'Binding of *Fusarium* mycotoxins by fermentative bacteria *in vitro*', *Journal of Applied Microbiology*, 101(4), 849–856.

Nielsen, T. R. H. *et al.* (2012) 'Antimicrobial activity of selected South African medicinal plants', *BMC Complementary and Alternative Medicine*, 12(1), 1086.

Nkomo, M. M. *et al.* (2014) 'Fusarium inhibition by wild populations of the medicinal plant *Salvia africana-lutea* L. linked to metabolomic profiling', *BMC Complementary and Alternative Medicine*, 14(1), 99.

Noruzi, M. (2015) 'Biosynthesis of gold nanoparticles using plant extracts', *Bioprocess and Biosystems Engineering*, 38(1), 1–14.

Olenic, L. *et al.* (2016) 'Chapter 18 GREEN NANOMATERIALS FOR PSORIATIC LESIONS in Nanomaterials and Regenerative Medicine', in, 477–508.

Rad, A. G., Abbasi, H. and Afzali, M. H. (2011) 'Gold Nanoparticles: Synthesising, Characterizing and Reviewing Novel Application in Recent Years', *Physics Procedia*, 22.

Savary, S. *et al.* (2018) 'Concepts, approaches, and avenues for modelling crop health and crop losses', *Recent advances in crop modelling to support sustainable agricultural production and food security under global change*, 100, 4–18.

Shakibaie, M., Salari Mohazab, N. and Ayatollahi Mousavi, S. A. (2015) 'Antifungal Activity of Selenium Nanoparticles Synthesized by *Bacillus* species Msh-1 Against *Aspergillus fumigatus* and *Candida albicans*', *Jundishapur Journal of Microbiology*, 8(9), e26381.

Sharma, P. *et al.* (2017) 'Nanomaterial Fungicides: In Vitro and In Vivo Antimycotic Activity of Cobalt and Nickel Nanoferrites on Phytopathogenic Fungi', *Global Challenges*, 1(9), 1700041.

Šišić, A. *et al.* (2018) 'Roots of symptom-free leguminous cover crop and living mulch species harbor diverse *Fusarium* communities that show highly variable aggressiveness on pea (*Pisum sativum*)', *PLOS ONE*, 13(2), e0191969.

Smith, I. M. *et al.* (eds) (1988) *European Handbook of Plant Diseases*. Oxford, UK: Blackwell Scientific Publications.

Staskawicz, B. J. (2001) 'Genetics of Plant-Pathogen Interactions Specifying Plant Disease Resistance', *Plant Physiology*, 125(1), 73–76.

Summerell, B. A. *et al.* (2010) 'Biogeography and phylogeography of *Fusarium*: a review', *Fungal Diversity: [Fungal Divers]*, 44, pp. 3–13.

Thuesombat, P. *et al.* (2014) 'Effect of silver nanoparticles on rice (*Oryza sativa* L. cv. KDML 105) seed germination and seedling growth', *Ecotoxicology and Environmental Safety*, 104, 302–309.

Topçu, G. (2006) 'Bioactive Triterpenoids from *Salvia* Species', *Journal of Natural Products*, 69(3), 482–487.

Venkatpurwar, V. and Pokharkar, V. (2011) 'Green synthesis of silver nanoparticles using marine polysaccharide: Study of in-vitro antibacterial activity', *Materials Letters - MATER LETT*, 65, 999–1002.

Vlaardingerbroek, I. *et al.* (2016) 'Dispensable chromosomes in *Fusarium oxysporum* f. sp. *lycopersici*', *Molecular Plant Pathology*, 17(9), 1455–1466.

Wang, Z. L. (2001) 'Characterization of Nanophase Materials', *Particle & Particle Systems Characterization*, 18(3), 142–165.

Wani, Ab. H. *et al.* (2011) 'In vitro inhibitory effect of fungicides and botanicals on mycelia growth and spore germination of *Fusarium oxysporum*', *J Biopes*, 4.

Watt, J. M. and Breyer-Brandwijk, M. G. (1962) 'The medicinal and poisonous plants of Southern and Eastern Africa'. Available at: <https://agris.fao.org/agris-search/search.do?recordID=XF2016015447>.

Wu, Y.-B. *et al.* (2012) 'Constituents from *Salvia* species and their biological activities', *Chemical Reviews*, 112(11), 5967–6026.

Yah, C. S. and Simate, G. S. (2015) 'Nanoparticles as potential new generation broad spectrum antimicrobial agents', *DARU Journal of Pharmaceutical Sciences*, 23(1), 43.

Youm, O. and Owusu, E. O. (1998) 'Farmers' perceptions of yield losses due to insect pests and methods for assessment in pearl millet', *International Journal of Pest Management*, 44(2), 123–125.

Zeilinger, S. *et al.* (2016) 'Friends or foes? Emerging insights from fungal interactions with plants', *FEMS microbiology reviews*, 40(2), 182–207.

Zhang, X. *et al.* (2018) 'Measurement and correlation of solubility of carbendazim in lower alcohols', *Thermochimica Acta*, 659, 172–175.